INTRODUCTION TO THE ELECTRONIC CORRELATION PROBLEM

PAUL E.S. WORMER

Institute of Theoretical Chemistry, University of Nijmegen, Toernooiveld, 6525 ED Nijmegen, The Netherlands

Contents

1 Introduction

These are notes for a six hour lecture series on the electronic correlation problem, given by the author at a Dutch national winterschool in 1999. The main purpose of this course was to give some theoretical background on the Møller-Plesset and coupled cluster methods. Both computational methods are available in many quantum chemical "black box" programs. The audience consisted of graduate students, mostly with an undergraduate chemistry education and doing research in theoretical chemistry.

A basic knowledge of quantum mechanics and quantum chemistry is presupposed. In particular a knowledge of Slater determinants, Slater-Condon rules and Hartree-Fock theory is a prerequisite of understanding the following notes. In Appendix A this theory is reviewed briefly.

Because of time limitations hardly any proofs are given, the theory is sketchily outlined. No attempt is made to integrate out the spin, the theory is formulated in terms of spin-orbitals only.

From the outset we make the following approximations:

- The clamped nuclei approximation. This is the removal of the nuclear kinetic energy terms from the Hamiltonian and the assumption that the wavefunction depends only on the electronic coordinates. Since the nuclear potential energy terms are *not* removed from the energy operator, the electronic wavefunction depends parametrically on the nuclear coordinates.

- No spin or relativistic interactions. For the lighter elements these are small and can, if necessary, be included via perturbation theory. For the heavier elements they are important.

Under these approximations the N-electron Hamiltonian becomes in atomic units ($m_e = 1, e = 1, \hbar = 1$)

$$H = \sum_{i=1}^{N} u(i) + \sum_{i>j} \frac{1}{r_{ij}} \quad \text{and} \quad u(i) \equiv -\frac{1}{2}\nabla_i^2 + \sum_{\alpha} \frac{Z_\alpha}{R_{\alpha i}}. \tag{1}$$

Here r_{ij} is the distance between electron i and j and $R_{\alpha i}$ between nucleus α with charge Z_α at position $\vec{R}_\alpha$ and electron i. Since the position vectors $\vec{R}_\alpha$ are taken to be constant, inclusion of the internuclear repulsions does not affect the eigenfunctions of the Hamiltonian in (1). It will give a constant shift in its eigenvalues.

Further we will restrict these lectures to closed-shell, ground state, spin-singlet molecules. We assume that for these systems the solution of the Hartree-Fock (HF) problem is available. As is well-known the HF equations follow from variation of the expectation value

$$E_{\rm HF} \equiv \langle\, \Phi_0 \,|\, H \,|\, \Phi_0 \,\rangle \tag{2}$$

where Φ_0 is a normalized Slater determinant (antisymmetrized product) containing the N lowest energy molecular spin-orbitals $\psi_i,\ i = 1 \ldots, N$. These so-called *occupied orbitals* are solutions of the HF equations and will be designated by $i, j, k, \ldots$. The solutions of the HF equations with energies higher than ϵ_N (the highest energy of the occupied orbitals) are the so-called *virtual spin-orbitals* and will be designated by $a, b, c, \ldots$.

We follow P.-O. Löwdin and define the *electronic correlation energy* ΔE_0 as the difference between $E_{\rm HF}$ and the lowest eigenvalue E_0 of the Hamiltonian (1)

$$\Delta E_0 = E_0 - E_{\rm HF}. \tag{3}$$

In other words, the electronic correlation problem is the problem of finding the lowest eigenvalue of the many-electron Schrödinger equation starting from the exact solutions of the corresponding HF equation.

Much work has been done on this problem. In the nineteen seventies and early eighties the configuration interaction (CI) method was developed to the extent that hundreds of thousands of configuration state functions (CSFs) can now be handled. Recall here that a CSF is a linear combination of Slater determinants that is an eigenfunction of the total spin operator S^2. Since S^2 commutes with H, the H-matrix will consist of blocks of different total spin quantum number S when CSFs are used.

It has been known in many-body physics since the nineteen fifties that most truncated CI methods are not *size extensive*. That is, if we compute M identical molecules with the interaction between the molecules switched off in the total M molecule Hamiltonian, we do not get M times the energy of one molecule computed with the same truncated CI method. We will see that this is due to the appearance of unlinked clusters in the CI energy. Goldstone's linked cluster theorem (1957) states that in an exact theory all unlinked clusters cancel each other. Although it was generally known that most CI methods yield non extensive energies, it was often ignored during the days that they were developed.

However, when it became clear that unlinked clusters do indeed give large unphysical contributions to CI energies, chemists turned to formalisms that are size extensive, notably Møller-Plesset (MP) perturbation theory and coupled cluster (CC) theory. These two methods, and variants thereof, are the most often applied today, at least for molecules near their equilibrium ground state. For molecules in excited non-singlet states and for dissociation processes the MP and CC approaches are generally not applicable, but CI is. We will give a short introduction to MP and coupled cluster theory. Since the concepts and language of perturbation theory are applied frequently in CC theory, we will start with the former formalism.

2 Rayleigh-Schrödinger perturbation theory

Rayleigh-Schrödinger perturbation theory (RSPT) can be fruitfully applied when we can partition our Hamiltonian H as follows:

$$H = H^{(0)} + V, \tag{4}$$

such that

1. We can compute the exact eigenvalues and eigenvectors of $H^{(0)}$. [Usually this requirement is too strong and we have to make do with (good) approximations of the eigenvalues and eigenvectors].

2. The spectrum of H is not too different from that of $H^{(0)}$. In other words the energy effects due to V are rather modest. That is why V is called a perturbation.

We consider $H(\lambda) \equiv H^{(0)} + \lambda V$ and its lowest energy eigenstate

$$H(\lambda)\Psi_0(\lambda) = E_0(\lambda)\Psi_0(\lambda), \tag{5}$$

which goes over into the problem to be solved when we choose $\lambda = 1$. We expand the exact solutions of $H(\lambda)$:

$$\Psi_0(\lambda) = \sum_{n=0}^{\infty} \lambda^n \Phi_0^{(n)} \quad \text{and} \quad E_0(\lambda) = \sum_{n=0}^{\infty} \lambda^n E_0^{(n)}. \tag{6}$$

Inserting these expansions into Eq. (5) and putting λ equal to zero, we get the *unperturbed* problem

$$H^{(0)} \,|\, \Phi_0^{(0)} \,\rangle = E_0^{(0)} \,|\, \Phi_0^{(0)} \,\rangle, \tag{7}$$

which we assume to be solved. Our goal is now to get expressions for the perturbation corrections $E_0^{(n)}$ and $\Phi_0^{(n)}$. We introduce the *intermediate normalization condition*:

$$\langle\, \Phi_0^{(0)} \,|\, \Phi_0^{(n)} \,\rangle = 0 \quad \text{for} \quad n > 0, \quad \text{and require} \quad \langle\, \Phi_0^{(0)} \,|\, \Phi_0^{(0)} \,\rangle = 1 \tag{8}$$

so that $\langle\, \Phi_0^{(0)} \,|\, \Psi_0(\lambda) \,\rangle = 1$. The exact lowest eigenvalue $E_0(\lambda)$ of $H(\lambda)$ satisfies then the equation

$$E_0(\lambda) - E_0^{(0)} = \lambda \langle\, \Phi_0^{(0)} \,|\, V \,|\, \Psi_0(\lambda) \,\rangle. \tag{9}$$

Upon expanding both sides of this equation, we find the *asymmetric energy expression* for the n^{th}-order energy

$$\boxed{E_0^{(n)} = \langle\, \Phi_0^{(0)} \,|\, V \,|\, \Phi_0^{(n-1)} \,\rangle} \quad n > 0. \tag{10}$$

We see that, if we know the $(n-1)^{\text{th}}$ order contribution to $\Psi_0(\lambda)$, we can compute the n^{th} order contribution to $E_0(\lambda)$. In particular, the first-order energy is the expectation value $E_0^{(1)} = \langle\, V \,\rangle$, where we have introduced the short hand notation $\langle\, Q \,\rangle = \langle\, \Phi_0^{(0)} \,|\, Q \,|\, \Phi_0^{(0)} \,\rangle$ for any operator Q.

The n^{th}-order perturbation equation is obtained by expanding $\Psi_0(\lambda)$ on both sides of the exact Schrödinger equation [Eq. (5)] and $E_0(\lambda)$ on the right hand side of this equation, followed by equating the terms on both sides that multiply λ^n. From the intermediate normalization condition follows that $\Phi_0^{(n)}$ can be obtained by solving the n^{th}-order equation (which is linear) on the orthogonal complement of $\Phi_0^{(0)}$. Using a basis of eigenfunctions of $H^{(0)}$ for this space, we introduce the *reduced resolvent*:

$$R \equiv \sum_{i>0} \frac{|\, \Phi_i^{(0)} \,\rangle \langle\, \Phi_i^{(0)} \,|}{E_0^{(0)} - E_i^{(0)}}, \tag{11}$$

which in fact is the inverse of $E_0^{(0)} - H^{(0)}$ in this particular representation. (Or more precisely, it is the inverse of the restriction of $E_0^{(0)} - H^{(0)}$ to the orthogonal complement of $\Phi_0^{(0)}$. Since the perturbation equations are linear, it is not surprising that this inverse enters the theory). We assume that the eigenvalues and eigenvectors of $H^{(0)}$ are known and hence we know R. Further we assume that $\Phi_0^{(0)}$ is non-degenerate.

As stated above, the recursion relation for the n^{th}-order perturbed function follows by equating terms in λ^n and dividing both sides by $E^{(0)} - H^{(0)}$,

$$|\, \Phi_0^{(n)} \,\rangle = RV \,|\, \Phi_0^{(n-1)} \,\rangle - \sum_{k=1}^{n} E_0^{(k)} R \,|\, \Phi_0^{(n-k)} \,\rangle. \tag{12}$$

The first-order correction to the wavefunction thus becomes

$$|\,\Phi_0^{(1)}\,\rangle = RV\,|\,\Phi_0^{(0)}\,\rangle \quad \text{hence} \quad E_0^{(2)} = \langle\,\Phi_0^{(0)}\,|\,V\,|\,\Phi_0^{(1)}\,\rangle = \langle\,VRV\,\rangle. \tag{13}$$

And

$$\begin{aligned} |\,\Phi_0^{(2)}\,\rangle &= RV\,|\,\Phi_0^{(1)}\,\rangle - E_0^{(1)}R\,|\,\Phi_0^{(1)}\,\rangle \\ &= RVRV\,|\,\Phi_0^{(0)}\,\rangle - \langle\,V\,\rangle R^2V\,|\,\Phi_0^{(0)}\,\rangle, \end{aligned} \tag{14}$$

so that

$$E_0^{(3)} = \langle\,\Phi_0^{(0)}\,|\,V\,|\,\Phi_0^{(2)}\,\rangle = \langle\,VRVRV\,\rangle - \langle\,V\,\rangle\langle\,VR^2V\,\rangle. \tag{15}$$

We can continue this recursion and derive $E^{(4)}$, etc. However, we will not do this but rather give general expressions for the perturbation energies by means of the bracketing technique of Brueckner. We will not attempt to prove why the technique works, but just give the recipe, which is very easy to apply. We will explain the procedure by the example of the fourth-order energy. We start with the expectation value of the operator product $\langle\,VRVRVRV\,\rangle$. (The perturbation V on the outside, the resolvents in between, four V's because we illustrate the fourth-order). The recipe then states that we must insert in all possible ways any number of bra and ket pairs such that they bracket V's and V's remain on the outside. A resolvent on the outside gives zero, since $R\,|\,\Phi_0^{(0)}\,\rangle = 0$ and $\langle\,\Phi_0^{(0)}\,|R = 0$. Thus, one pair can be placed as follows

$$\begin{aligned} \langle\,VR\langle\,V\,\rangle RVRV\,\rangle &= \langle\,V\,\rangle\langle\,VR^2VRV\,\rangle \\ \langle\,VRVR\langle\,V\,\rangle RV\,\rangle &= \langle\,V\,\rangle\langle\,VRVR^2V\,\rangle \\ \langle\,VR\langle\,VRV\,\rangle RV\,\rangle &= \langle\,VR^2V\,\rangle\langle\,VRV\,\rangle. \end{aligned} \tag{16}$$

Also two pairs of brackets may be inserted, provided they are properly nested

$$\langle\,VR\langle\,V\,\rangle R\langle\,V\,\rangle RV\,\rangle = \langle\,VR^3V\,\rangle\langle\,V\,\rangle\langle\,V\,\rangle. \tag{17}$$

Each term gets the sign $(-1)^{\#}$ where $\#$ is the number of pairs and we sum the signed terms. Summarizing, we find by the bracketing technique the following perturbation energies through fourth-order:

$$\begin{aligned} E_0^{(1)} &= \langle\,V\,\rangle \\ E_0^{(2)} &= \langle\,VRV\,\rangle \\ E_0^{(3)} &= \langle\,VRVRV\,\rangle - \langle\,VR^2V\,\rangle\langle\,V\,\rangle \\ E_0^{(4)} &= \langle\,VRVRVRV\,\rangle - \langle\,V\,\rangle\langle\,VR^2VRV\,\rangle - \langle\,V\,\rangle\langle\,VRVR^2V\,\rangle \\ &\quad -\langle\,VR^2V\,\rangle\langle\,VRV\,\rangle + \langle\,VR^3V\,\rangle\langle\,V\,\rangle\langle\,V\,\rangle. \end{aligned} \tag{18}$$

In fifth-order we find for the first time a bracket within a bracket:

$$\langle\, VR\langle\, VR\langle\, V\,\rangle RV\,\rangle RV\,\rangle$$

which obtains a plus sign (two pairs). In higher order it is easy to overlook certain pairings and therefore the following formula for the number of terms appearing in n^{th}-order gives a useful check

$$\# = \frac{(2n-2)!}{n!(n-1)!}. \tag{19}$$

3 Møller-Plesset perturbation theory

One could describe Møller-Plesset perturbation theory as RSPT with

$$H^{(0)} \equiv F = \sum_{i=1}^{N} f(i) \quad \text{and} \quad V \equiv H - F. \tag{20}$$

Here F, the total Fock operator, is the zeroth order Hamiltonian and the *correlation operator* $H - F$ is the perturbation.

Actually, a slightly different partitioning of the exact H is more convenient:

$$H = \overbrace{F + \langle\, H - F\,\rangle}^{H^{(0)}} + \overbrace{H - F - \langle\, H - F\,\rangle}^{V}, \tag{21}$$

which defines $H^{(0)}$ and the correlation operator V, respectively. Using the perturbation equations (18) we find the Møller-Plesset (MP) energies through fourth-order

$$\begin{aligned}
E_0^{(0)} &= \langle\, H^{(0)}\,\rangle = \langle\, H\,\rangle = E_{\text{HF}} \\
E_0^{(1)} &= 0 \\
E_0^{(2)} &= \langle\, VRV\,\rangle \\
E_0^{(3)} &= \langle\, VRVRV\,\rangle \\
E_0^{(4)} &= \langle\, VRVRVRV\,\rangle - \langle\, VR^2V\,\rangle\langle\, VRV\,\rangle.
\end{aligned} \tag{22}$$

The fourth-order energy is the first where a renormalization term, namely $\langle\, VR^2V\,\rangle\langle\, VRV\,\rangle$, appears.

In Appendix A it is shown that the unperturbed (zeroth-order) functions are Slater determinants built from eigenfunctions of the one-electron Fock operator $f(1)$, the so-called canonical HF orbitals.

We drop from here on the subscript 0, since we are only concerned with the correlation of the ground state, and consider $E^{(2)} = \langle\, VRV \,\rangle$. The resolvent R consists in this case of a sum over singly excited states plus a sum over doubly excited states ..... plus a sum over N-tuply excited states. By virtue of Brillouin's theorem, (see Appendix A), the singly excited states do not contribute. Since the perturbation V contains at most two-electron operators, it follows from the Slater-Condon rules that higher than double excitations do not contribute. Hence

$$E^{(2)} = \frac{1}{4} \sum_{i,j,a,b} \frac{|\langle\, \Phi_0 \,|\, V \,|\, \Phi_{ij}^{ab} \,\rangle|^2}{\epsilon_i + \epsilon_j - \epsilon_a - \epsilon_b}, \tag{23}$$

where we used that the energy of Φ_0 is $E_{\rm HF}$. The energy of Φ_{ij}^{ab} is $E_{\rm HF} - \epsilon_i - \epsilon_j + \epsilon_a + \epsilon_b$. The factor $1/4$ is due to the overcompleteness of the basis. Since a linearly independent basis requires $i > j$ and $a > b$ and we do not apply this condition, we correct by $1/4$. Notice also that $\Phi_{ij}^{aa} = 0$ and that one defines $\Phi_{ii}^{ab} = 0$ in a second quantized formalism, so that the diagonal cases do not enter.

We introduce the shorthand notation

$$\langle pq||rs\rangle \equiv \langle\, \psi_p(1)\psi_q(2) \,|\, (1 - P_{12})/r_{12} \,|\, \psi_r(1)\psi_s(2) \,\rangle.$$

By the Slater-Condon rules we find for this case of two mismatches between bra and ket:

$$\begin{aligned} \langle\, \Phi_0 \,|\, H \,|\, \Phi_{ij}^{ab} \,\rangle &= \langle ij||ab\rangle, \\ \langle\, \Phi_0 \,|\, F \,|\, \Phi_{ij}^{ab} \,\rangle &= \langle\, \Phi_0 \,|\, \Phi_{ij}^{ab} \,\rangle = 0 \end{aligned} \tag{24}$$

and the second-order MP energy becomes

$$E^{(2)} = \frac{1}{4} \sum_{i,j,a,b} \frac{\langle ij||ab\rangle\langle ab||ij\rangle}{\epsilon_i + \epsilon_j - \epsilon_a - \epsilon_b}. \tag{25}$$

It is possible to express the third- and fourth-order MP energies in Eq. (22) by the aid of the Slater-Condon rules in terms of two-electron integrals and orbital energies only. In third-order we will meet matrix elements of the kind $\langle\, \Phi_{ij}^{ab} \,|\, H - F - \langle\, H - F \,\rangle \,|\, \Phi_{i'j'}^{a'b'} \,\rangle$. The Fock operator, being a sum of one-electron operators, only contributes in the case of less than two mismatches between bra and ket. These Fock matrix elements cancel exactly against the corresponding terms arising from the two-electron part of H. In other words,

we do not find contributions from the Fock operator in the MP energies. This is true in all orders of MP theory, as long as canonical HF orbitals are used. This fact is self-evident in the second quantized hole-particle approach to MP perturbation theory, (see Paldus & Čížek).

4 Diagrammatic perturbation theory

An alternative to the Slater-Condon rules is the use of diagrams. Basically there are two closely related type of many-body diagrams: Hugenholtz and Goldstone. Both are inspired by Feynman diagrams, which arise in time-dependent perturbation theory. The theory starts from a Fermi vacuum state $|\,\Phi_0\,\rangle$, which simply is the lowest eigenfunction of F (all occupied orbitals filled). When we promote an electron to a virtual orbital we create a hole in the Fermi vacuum and a particle in a virtual orbital. Thus, e.g. the Slater determinant Φ_{ij}^{ab} is a 2-hole/2-particle state. One says that the holes 'run backwards in time' and the particles 'run forward'. In the present time-independent approach this is just a rule of thumb to remember the orientation of lines in the diagrams.

There are two conventions of drawing Goldstone and Hugenholtz diagrams: (i) Time flows from right to left. (ii) Time flows from bottom to top. We will use the first convention, which is to say that *hole lines run from left to right and particle lines from right to left.* We will first restrict the attention to Hugenholtz diagrams, because they are easiest to draw.

The basic building block is the antisymmetrized two-electron integral:

$\langle pq||rs\rangle \longrightarrow$ 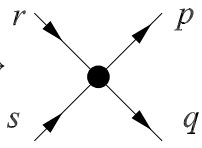

(26)

where *the orbitals in the bra leave the vertex and the orbitals in the ket enter the vertex.* Here p, q, r, s are arbitrary orbitals. If we make a choice for occupied and virtual orbitals we must direct the lines either to the right (holes: $i, j, \cdots$) or to the left (particles: $a, b, \cdots$). Thus, a product of two antisymmetric integrals becomes,

$\langle ij||ab\rangle\langle ab||ij\rangle \longrightarrow$ 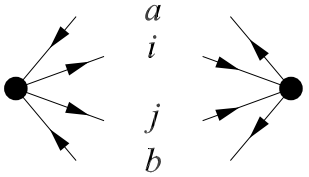

The energy denominator is sometimes given by a vertical line. For the case of an intermediate doubly excited state it is:

$$(\epsilon_i + \epsilon_j - \epsilon_a - \epsilon_b)^{-1} \longrightarrow$$

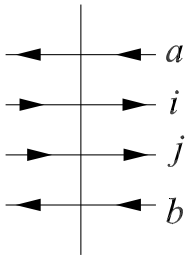

Combining these ingredients we get for the second-order MP energy, where the labels of closed lines are summed over:

$$\frac{1}{4}\sum_{i,j,a,b}\frac{\langle ij||ab\rangle\langle ab||ij\rangle}{\epsilon_i + \epsilon_j - \epsilon_a - \epsilon_b} \longrightarrow$$

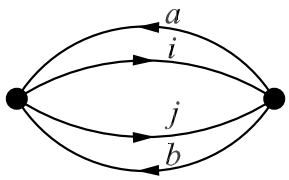

It is common not to show the vertical line cutting the lines in between the vertices that denotes the energy denominator, which is why we do not show it here.

It remains to explain how we can extract the factor 1/4 from the diagram. Two lines are *equivalent* when both start and end at the same vertex and both go in the same direction. Let k be the number of pairs of equivalent lines in the diagram. Then we must multiply the diagram with a weight factor $(1/2)^k$. In the present case we have one equivalent pair of hole lines and one pair of equivalent particle lines, hence $k = 2$.

We summarize the graphical rules:

1. For an n^{th}-order energy we write n vertices on a horizontal line. Each vertex has two ingoing (say r and s) and two out going lines (say p and q). Such a vertex contributes $\langle pq||rs\rangle$.

2. Connect these vertices in all possible ways such that the resulting diagram is linked (see below). A vertex may not be connected with itself. Each distinct diagram gives a separate algebraic term. The n^{th} order energy is the sum of these terms.

3. Between each pair of vertices we draw a virtual vertical line. This gives the denominator factor

$$\sum_{\text{holes}} \epsilon_i - \sum_{\text{particles}} \epsilon_a \tag{27}$$

where the sum runs over all hole and particle lines crossing the virtual line.

4. Sum over the labels of all hole and particle lines.

5. Multiply by the weight factor 2^{-k}, where k is the number of pairs of equivalent lines.

6. Multiply by the correct sign (see below).

We will demonstrate the method on the third-order energy. First we draw all the possible skeleton (i.e. without arrows) diagrams. In this case there is only one possibility

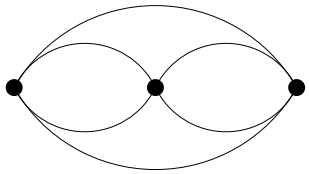

The above rules exclude the following third-order diagram because it contains a vertex connected with itself:

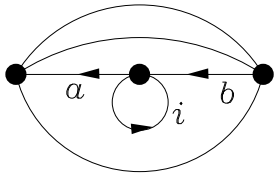

This diagram contains $\sum_i \langle ai||bi\rangle = \langle\, a \,|\, f - u \,|\, b \,\rangle$. See Eqs. (1) and (83) for the definitions of u and f. As discussed above this two-electron part of the Fock operator cancels against some two-electron terms, and that is why our diagrammatic rules do not allow these diagrams.

Secondly, we insert all arrows in all possible ways. After a moment's reflection we see that there are three possibilities: the outside lines can (i) both run to the left (ii) both run to the right or (iii) run in different directions.

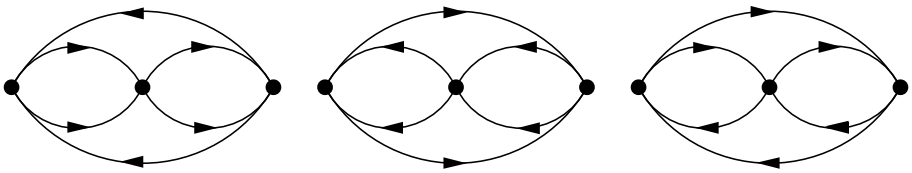

Algebraically the corresponding third-order MP energies are (up to sign):

$$
\begin{aligned}
E_{(i)} &= \pm\frac{1}{8}\sum_{i,j,k,l,a,b}\frac{\langle ij||ab\rangle\langle kl||ij\rangle\langle ab||kl\rangle}{(\epsilon_i+\epsilon_j-\epsilon_a-\epsilon_b)(\epsilon_k+\epsilon_l-\epsilon_a-\epsilon_b)} \\
E_{(ii)} &= \pm\frac{1}{8}\sum_{a,b,c,d,i,j}\frac{\langle ij||ab\rangle\langle ab||cd\rangle\langle cd||ij\rangle}{(\epsilon_i+\epsilon_j-\epsilon_a-\epsilon_b)(\epsilon_i+\epsilon_j-\epsilon_c-\epsilon_d)} \\
E_{(iii)} &= \pm\sum_{a,b,c,i,j,k}\frac{\langle ij||ab\rangle\langle ak||ci\rangle\langle bc||jk\rangle}{(\epsilon_i+\epsilon_j-\epsilon_a-\epsilon_b)(\epsilon_j+\epsilon_k-\epsilon_b-\epsilon_c)}.
\end{aligned}
\tag{28}
$$

We now turn to the sign rule. Hugenholtz diagrams do no specify the overall sign of the contribution of the diagram. This is due to the fact that the basic diagram (26) may represent $\langle pq||rs\rangle$ as well as $\langle pq||sr\rangle$, which differ in sign. In order to fix the sign it is necessary to distinguish the two particles participating in the interaction. We follow the suggestion of Brandow and draw one Goldstone representative of each Hugenholtz diagram. That is, each vertex is replaced as follows

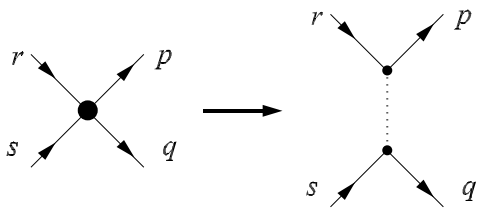

Now, orbital r and p are occupied by one electron, say electron 1, and s and q by the other (electron 2). Hence the diagram gives unambiguously $\langle\psi_p(1)\psi_q(2)||\psi_r(1)\psi_s(2)\rangle$. The Goldstone diagram on the right hand side is in fact a Feynman diagram describing the exchange of a photon (dashed line) between electron 1 and 2. Since we work in a non-relativistic framework, the interaction is instantaneous, which is why the dashed line is vertical (remember that the time axis is horizontal).

In order to obtain a Goldstone representative from a Hugenholtz diagram we replace all nodes as above, while keeping the directions of the lines and the connectivity intact. Usually more than one possibility exists. For instance the first third-order diagram above has two representatives:

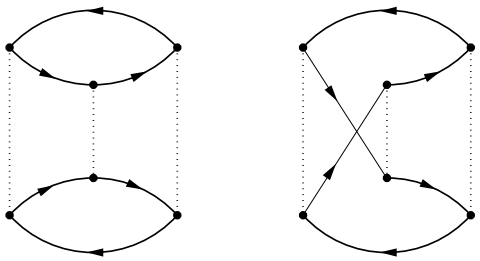

Note that the first representative contains two loops. A loop contains oriented non-dashed (= orbital) lines which, when followed starting at a certain vertex, bring us back to this vertex. The second diagram has one loop. Let the number of loops be l. Let the number of hole lines in a certain diagram be h (both diagrams have $h = 4$). Then the overall sign is $(-1)^{l+h}$. So the first representative has sign $+1$ and the numerator

$$\langle ij||ab\rangle\langle kl||ij\rangle\langle ab||kl\rangle$$

while the second has sign -1 and the numerator

$$\langle ij||ab\rangle\langle kl||ji\rangle\langle ab||kl\rangle.$$

Since $\langle kl||ji\rangle = -\langle kl||ij\rangle$ we see that both representatives give indeed the same result.

The third-order diagram (iii) has eight different representatives, but again only one is needed, for instance the following one

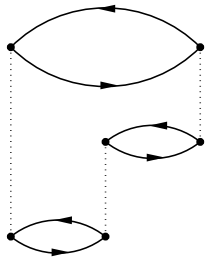

which has $l = 3$ and $h = 3$. Hence this diagram yields the contribution

$$\begin{aligned} E_{(iii)} &= \sum_{a,b,c,i,j,k} \frac{\langle ij||ab\rangle\langle ak||ic\rangle\langle bc||jk\rangle}{(\epsilon_i + \epsilon_j - \epsilon_a - \epsilon_b)(\epsilon_j + \epsilon_k - \epsilon_b - \epsilon_c)} \\ &= -\sum_{a,b,c,i,j,k} \frac{\langle ij||ab\rangle\langle ak||ci\rangle\langle bc||jk\rangle}{(\epsilon_i + \epsilon_j - \epsilon_a - \epsilon_b)(\epsilon_j + \epsilon_k - \epsilon_b - \epsilon_c)} \end{aligned} \tag{29}$$

Recall that the horizontal axis is a time axis, so that every one of the n vertices in a MPn diagram has a definite time value, counting from left to right: $t_1 > t_2 > \cdots > t_n$. Evidently, these time values do not change if we move the nodes along vertical lines. Inspecting the graphical rules (3)–(6) we see that the value of a diagram is unaffected by such a deformation. In fact, quite some left-right motion is also allowed *as long as the time ordering of the nodes is not changed*. As soon as we change the time ordering of the nodes we get a different diagram: *a different time version*. For example, the diagrams

(A), (B) and (C) are the same (and only one of them must be included in the total MP4 energy) whereas diagram (D) is a different time-version and must be included:

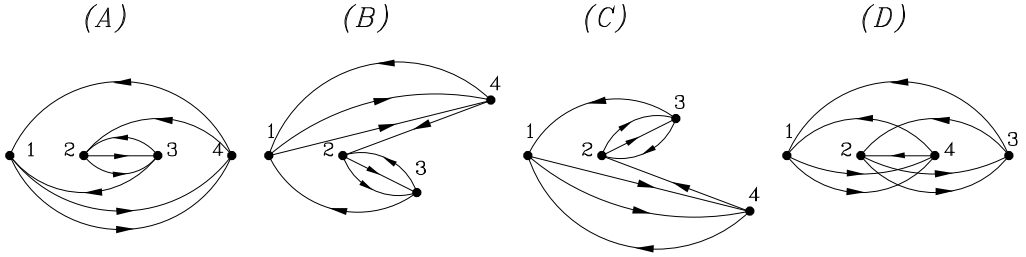

(30)

So, the first graphical rule, which stated that the vertices must be on one horizontal line, was formulated too strictly.

5 Unlinked clusters

The fourth-order renormalization term [see Eq. (22)] is an example of an unlinked cluster. Diagrammatically it reads

$$\langle\, VR^2V \,\rangle\langle\, VRV \,\rangle \rightarrow$$

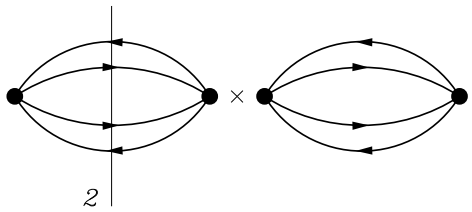

(31)

The vertical line indicates the denominator squared, so that algebraically

$$\begin{aligned} \langle\, VR^2V \,\rangle\langle\, VRV \,\rangle \;&=\; \frac{1}{16}\left(\sum_{i,j,a,b}\frac{|\langle ij||ab\rangle|^2}{(\epsilon_i+\epsilon_j-\epsilon_a-\epsilon_b)^2}\right) \\ &\quad\times\left(\sum_{i,j,a,b}\frac{|\langle ij||ab\rangle|^2}{\epsilon_i+\epsilon_j-\epsilon_a-\epsilon_b}\right). \end{aligned} \tag{32}$$

Note that $\langle\, VR^2V \,\rangle = \langle\, \Phi^{(1)} \,|\, \Phi^{(1)} \,\rangle$ and hence is positive, whereas $\langle\, VRV \,\rangle$ is negative.

We mentioned in the introduction that unlinked clusters break size extensivity. To explain this we assume that we are considering a system consisting of two non-interacting subsystems A and B. Let the spin-orbitals $p', q', \ldots$ be centered on A and $p'', q'', \ldots$ be on B. By this assumption the differential overlap of any spin-orbital on A with any one on B is zero, so that two-center

integrals of e.g. the type $\langle p''q'||r's'\rangle$ are zero. Hence the second-order energy becomes

$$\frac{1}{4}\sum_{i',j',a',b' \text{ on A}} \frac{|\langle i'j'||a'b'\rangle|^2}{\epsilon_{i'}+\epsilon_{j'}-\epsilon_{a'}-\epsilon_{b'}} + \frac{1}{4}\sum_{i'',j'',a'',b'' \text{ on B}} \frac{|\langle i''j''||a''b''\rangle|^2}{\epsilon_{i''}+\epsilon_{j''}-\epsilon_{a''}-\epsilon_{b''}} \quad (33)$$

which is the sum of the second-order energies of A and B. In other words, the second-order energy is size extensive. If we now look at Eq. (32), we see that terms of the kind

$$\left(\sum_{i',j',a',b' \text{ on A}} \frac{|\langle i'j'||a'b'\rangle|^2}{(\epsilon_{i'}+\epsilon_{j'}-\epsilon_{a'}-\epsilon_{b'})^2}\right) \times \left(\sum_{i'',j'',a'',b'' \text{ on B}} \frac{|\langle i''j''||a''b''\rangle|^2}{\epsilon_{i''}+\epsilon_{j''}-\epsilon_{a''}-\epsilon_{b''}}\right). \quad (34)$$

are non-vanishing. Because these terms are all negative they cannot cancel each other. So, even though A and B do not interact these non-vanishing bilinear energy terms are present and contribute to the energy of the dimer.

In this connection it is of interest to remark that exactly these terms pollute the DCI (configuration interaction based on doubly excited states) energy $E_{\rm D}$. In order to show this we choose as the energy zero

$$\langle\, H^{(0)}\,\rangle = \langle\, H\,\rangle = E_{\rm HF} = 0.$$

We write

$$E_{\rm D} \approx \frac{\langle\, \Phi^{(0)}+\Phi^{(1)} \,|\, H^{(0)}+V \,|\, \Phi^{(0)}+\Phi^{(1)}\,\rangle}{\langle\, \Phi^{(0)}+\Phi^{(1)} \,|\, \Phi^{(0)}+\Phi^{(1)}\,\rangle}, \quad (35)$$

or, using that $\langle\, \Phi^{(0)}+\Phi^{(1)} \,|\, \Phi^{(0)}+\Phi^{(1)}\,\rangle = 1+\langle\, \Phi^{(1)} \,|\, \Phi^{(1)}\,\rangle$,

$$E_{\rm D} = -E_{\rm D}\langle\, \Phi^{(1)} \,|\, \Phi^{(1)}\,\rangle + \langle\, \Phi^{(0)} \,|\, V \,|\, \Phi^{(1)}\,\rangle + \langle\, \Phi^{(1)} \,|\, V \,|\, \Phi^{(0)}\,\rangle + \langle\, \Phi^{(1)} \,|\, H^{(0)} \,|\, \Phi^{(1)}\,\rangle, \quad (36)$$

where we omitted the third-order term $\langle\, \Phi^{(1)} \,|\, V \,|\, \Phi^{(1)}\,\rangle$. Since $H^{(0)}R = -1$ we find

$$H^{(0)} \,|\, \Phi^{(1)}\,\rangle = H^{(0)}RV \,|\, \Phi^{(0)}\,\rangle = -V \,|\, \Phi^{(0)}\,\rangle$$

so that

$$\langle\, \Phi^{(1)} \,|\, H^{(0)} \,|\, \Phi^{(1)}\,\rangle = -\langle\, \Phi^{(1)} \,|\, V \,|\, \Phi^{(0)}\,\rangle.$$

If we replace on the right hand side of Eq. (36) $E_{\rm D}$ by $E^{(2)} = \langle\, \Phi^{(0)} \,|\, V \,|\, \Phi^{(1)}\,\rangle$ we find for the DCI energy

$$E_{\rm D} \approx E^{(2)} - \langle\, \Phi^{(1)} \,|\, \Phi^{(1)}\,\rangle E^{(2)}. \quad (37)$$

The second term is represented by the diagram in Eq. (31).

Given a normalized DCI vector $C_0(\Phi^{(0)} + \Phi^{(1)})$ it is easy to find an expression for $\langle\, \Phi^{(1)} \,|\, \Phi^{(1)} \,\rangle$. Indeed,

$$1 = C_0^2 \langle\, \Phi^{(0)} + \Phi^{(1)} \,|\, \Phi^{(0)} + \Phi^{(1)} \,\rangle = C_0^2 (1 + \langle\, \Phi^{(1)} \,|\, \Phi^{(1)} \,\rangle)$$

so that

$$\langle\, \Phi^{(1)} \,|\, \Phi^{(1)} \,\rangle = \frac{(1 - C_0^2)}{C_0^2}$$

The term $E_{\rm D}(1 - C_0^2)/C_0^2$ is the *Davidson-Siegbahn size-consistency correction*. Note that C_0 is the coefficient of the HF ground state in the normalized DCI vector.

We stated above that only linked clusters have to be considered in MP perturbation theory. Indeed, the renormalization terms cancel against the unlinked clusters that appear in $\langle\, VRVRVRV \,\rangle$. It is easily seen that the following two diagrams are the only unlinked possibilities appearing in $\langle\, VRVRVRV \,\rangle$, because a third time version, with the upper diagram sticking out to the left of the lower one, is the same as the first one. (Recall that the nodes may be moved vertically).

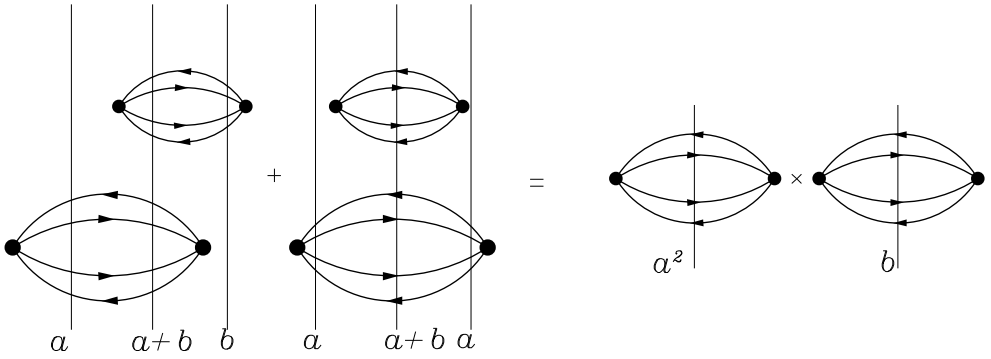

(38)

Schematically we have indicated the denominators. Noticing that all diagrams have the same numerator and using for the denominators

$$\frac{1}{a}\frac{1}{(a+b)}\frac{1}{b} + \frac{1}{a}\frac{1}{(a+b)}\frac{1}{a} = \frac{1}{a^2 b} \tag{39}$$

we find Eq. (38). The terms on the right hand side of this equation cancel exactly the fourth-order renormalization term. Note further that the diagrams on the left hand side of Eq. (38) are derived from intermediate quadruply excited states (the middle vertical line crosses four hole-particle pairs), which is why in DQCI the 'Davidson-Siegbahn' unlinked cluster does not appear.

So, we have shown for the special case of fourth-order Møller-Plesset theory that unlinked clusters cancel. This is a general result known as the *linked cluster theorem*:

$$\Delta E \equiv E - E_{\rm HF} = \sum_{n=0}^{\infty} \langle \, \{V(RV)^n\}_{\rm L} \, \rangle \tag{40}$$

That is, we sum over all orders and retain in every order only the linked diagrams. This restriction on the sum is indicated by the subscript L. In the proof of this theorem one shows that in all orders unlinked clusters and renormalization terms cancel each other. It follows that MP perturbation theory is size extensive in all orders. Note that the number of linked Hugenholtz diagrams grows quickly as a function of order. From first through sixth order the numbers of linked diagrams are 0, 1, 3, 39, 840, and 28300.

6 Convergence of MP perturbation theory

D. Cremer and Z. He published some convergence studies [J. Phys. Chem. **100**, 6173 (1996)]. They distinguish class A and class B molecules. Class A consists of BH, NH_2, CH_3, and CH_2. All molecules are considered at different geometries. The class A molecules are systems with well-separated electron pairs. Class B consists of Ne, F, F^- and hydrogen fluoride again at different geometries. Class B molecules are systems with electron clustering. Cremer and He compare the MP results with full CI results in the same basis. Full CI is based on all possible Slater determinants (ground+singly+ doubly+$\cdots$+ N-tuply excited) and hence is exact *within the given AO basis*. Of course, truncation of the AO basis introduces a serious error. However, within a given basis full CI can serve as a benchmark.

Cremer and He show that on the average the class A molecules have a monotonic convergence:

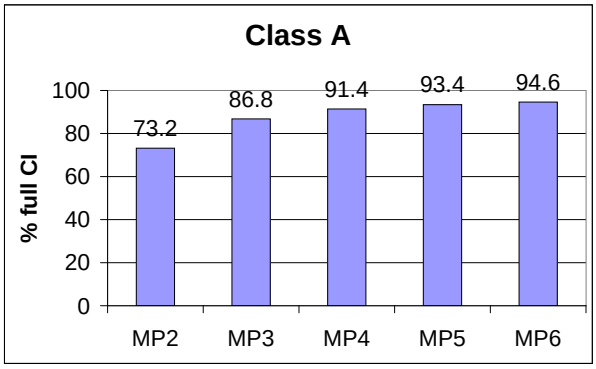

The class B molecules show a more oscillatory behavior:

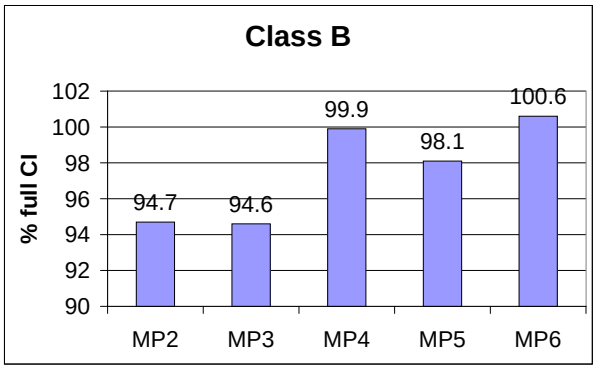

Note that MP6 overshoots the 100% mark, which is not forbidden as perturbation theory is non-variational.

7 Second quantization

In order to discuss the coupled cluster (CC) method we will need the k-fold excitation operator $E^{a_1 a_2 \cdots a_k}_{i_1 i_2 \cdots i_k}$, which is the operator that replaces in the unperturbed HF function Φ_0 the spin-orbital ψ_{i_1} by ψ_{a_1}, ψ_{i_2} by ψ_{a_2}, etc. Although a first quantized definition of this operator is possible, it is fairly cumbersome, while in second quantization its definition is most natural. So, it is convenient to introduce at this point the second quantization formalism.

We define the operator $X^\dagger_p$ that creates an electron in spin-orbital ψ_p and its hermitian conjugate X_p that annihilates an electron in spin-orbital ψ_p.

Antisymmetry imposes the anticommutation relations $\{A, B\} \equiv AB + BA$:

$$\left\{X_p^\dagger, X_q^\dagger\right\} = \{X_p, X_q\} = 0 \text{ and } \left\{X_q, X_p^\dagger\right\} = \left\{X_p^\dagger, X_q\right\} = \langle\, \psi_p \,|\, \psi_q \,\rangle = \delta_{pq}. \tag{41}$$

In second quantization the ground state Slater determinant can be written as

$$|\, \Phi_0 \,\rangle \equiv X_{i_1}^\dagger X_{i_2}^\dagger \ldots X_{i_N}^\dagger \,|\, 0 \rangle,$$

where $|\, 0 \,\rangle$ is the vacuum state, i.e. $X_p \,|\, 0 \,\rangle = 0$ and $X_p^\dagger \,|\, 0 \,\rangle = |\, \psi_p \,\rangle$. We define

$$E_{q_1 q_2 \cdots q_k}^{p_1 p_2 \cdots p_k} = X_{p_1}^\dagger X_{p_2}^\dagger \ldots X_{p_k}^\dagger X_{q_k} X_{q_{k-1}} \ldots X_{q_1}. \tag{42}$$

for arbitrary orbital labels $p_1, \ldots, p_k$ and $q_1, \ldots, q_k$. One-electron operators have in second quantization the form

$$U = \sum_{p,q} \langle\, p \,|\, u \,|\, q \,\rangle E_q^p, \tag{43}$$

while two-electron operators have the form

$$V = \frac{1}{2} \sum_{p_1 p_2 q_1 q_2} \langle\, p_1 p_2 \,|\, v \,|\, q_1 q_2 \,\rangle E_{q_1 q_2}^{p_1 p_2} = \frac{1}{4} \sum_{p_1 p_2 q_1 q_2} \langle p_1 p_2 || q_1 q_2 \rangle E_{q_1 q_2}^{p_1 p_2}. \tag{44}$$

One can prove a priori that the one- and two-electron operators have this form, or one can check a posteriori that these operators have the same matrix elements in the space of Slater determinants as their first-quantized counterparts. We skip both proofs.

The *k-fold excitation operator* is $E_{i_1 i_2 \cdots i_k}^{a_1 a_2 \cdots a_k}$, i.e. the upper indices are virtual orbitals and the lower indices are occupied orbitals. Excitation operators commute and can be factorized, for example,

$$E_{i_1 i_2}^{a_1 a_2} = E_{i_1}^{a_1} E_{i_2}^{a_2} = E_{i_2}^{a_2} E_{i_1}^{a_1}. \tag{45}$$

This follows directly from the anticommutation relations and the fact that occupied and virtual orbitals are orthogonal, in other words $\delta_{a_1 i_1} = 0$, so that

$$\begin{aligned} E_{i_1 i_2}^{a_1 a_2} &= X_{a_1}^\dagger X_{a_2}^\dagger X_{i_2} X_{i_1} = -X_{a_1}^\dagger X_{a_2}^\dagger X_{i_1} X_{i_2} = X_{a_1}^\dagger X_{i_1} X_{a_2}^\dagger X_{i_2} - \delta_{a_2 i_1} X_{a_1}^\dagger X_{i_2} \\ &= E_{i_1}^{a_1} E_{i_2}^{a_2}. \end{aligned} \tag{46}$$

We show that indeed $E_{i_1 i_2 \cdots i_k}^{a_1 a_2 \cdots a_k}$ is an excitation operator and consider

$$E_{i_1 i_2 \cdots i_k}^{a_1 a_2 \cdots a_k} \,|\, \Phi_0 \,\rangle = E_{i_1 i_2 \cdots i_{k-1}}^{a_1 a_2 \cdots a_{k-1}} E_{i_k}^{a_k} X_{i_1}^\dagger X_{i_2}^\dagger \ldots X_{i_N}^\dagger \,|\, 0 \rangle. \tag{47}$$

Move $E^{a_k}_{i_k}$ to the right until it hits $X^\dagger_{i_k}$. Since we commute a pair, no sign is changed: $E^{a_k}_{i_k} X^\dagger_i = X^\dagger_i E^{a_k}_{i_k}$ for $i \neq i_k$. When we hit $X^\dagger_{i_k}$ we leave $X^\dagger_{a_k}$ behind and use $X_{i_k} X^\dagger_{i_k} = -X^\dagger_{i_k} X_{i_k} + 1$. The first term vanishes because X_{i_k} may be moved further to the right until it reaches $|\,0\,\rangle$ and $X_{i_k}\,|\,0\,\rangle = 0$. So we find $X^\dagger_{a_k}$ at the position where before $X^\dagger_{i_k}$ was. At the same time we removed $E^{a_k}_{i_k}$ from the excitation operator. Then we do the same with $E^{a_{k-1}}_{i_{k-1}}$ and so on.

Note that

$$E^{a_1 \cdots i \cdots a_k}_{i_1 \cdots i_k}\,|\,\Phi_0\,\rangle = E^{a_1 \cdots a_k}_{i_1 \cdots a \cdots i_k}\,|\,\Phi_0\,\rangle = 0 \tag{48}$$

because on the left hand side an electron is created in an orbital (i) that is already occupied in Φ_0 and in the middle equation an electron is annihilated in an orbital (a) that is not occupied in Φ_0.

We associate $X^\dagger_p\,|\,\Phi_0\,\rangle$ with a free line leaving a diagram and $X_q\,|\,\Phi_0\,\rangle$ with a free line entering a diagram and we see that $E^{a_1 \cdots a_k}_{i_1 \cdots i_k}\,|\,\Phi_0\,\rangle$ is represented by a diagram with only lines sticking out to the left. Namely, a line sticking out to the right and leaving the diagram stands for $X^\dagger_i\,|\,\Phi_0\,\rangle = 0$ and likewise one entering on the right stands for $X_a\,|\,\Phi_0\,\rangle = 0$. A line leaving the diagram from the left stands for a particle creator $X^\dagger_a$ and one entering on the left for a hole creator (a particle annihilator) X_i, i.e. $E^a_i\,|\,\Phi_0\,\rangle$ is indeed represented by two lines sticking out to the left. Note parenthetically that $E^{ab}_{ii}\,|\,\Phi_0\,\rangle = E^{aa}_{ij}\,|\,\Phi_0\,\rangle = 0$, a fact that we mentioned earlier. Thus, the diagrammatic rules are extended to wavefunctions: Free lines are associated with creation and annihilation operators acting on Φ_0, while vertices are associated with antisymmetric integrals in the same way as for energy diagrams.

As a first example we consider the first order contribution $\Phi^{(1)}$, which is expanded in doubly excited Slater determinants

$$\Phi^{(1)} = RV\,|\,\Phi_0\,\rangle = \frac{1}{4}\sum_{a,b,i,j} \frac{E^{ab}_{ij}\,|\,\Phi_0\,\rangle\langle ab||ij\rangle}{\Delta^{ab}_{ij}}. \tag{49}$$

Here $\Delta^{ab}_{ij} = \epsilon_i + \epsilon_j - \epsilon_a - \epsilon_b$. Algebraically, the factor $1/4$ is again due to the overcompleteness of the basis when we do not apply the restrictions $a > b$ and $i > j$. Depicted as a Hugenholtz diagram or its Goldstone representative

(Brandow diagram) the sum is:

$$\frac{1}{4}\sum_{i,j,a,b}\frac{E_{ij}^{ab}\,|\,\Phi_0\,\rangle\langle ab||ij\rangle}{\Delta_{ij}^{ab}} =$$

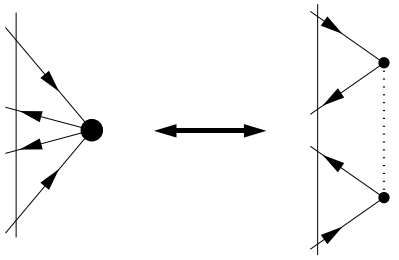

, (50)

with $E_{ij}^{ab} = X_a^\dagger X_b^\dagger X_j X_i$. Diagrammatically the factor 1/4 is due to the two pairs of equivalent lines sticking out. Equivalent means that the free lines are attached to the same Hugenholtz vertex and are of the same type (particle or hole). As a new diagrammatic rule we find that the free lines sticking out to the left are crossed by a (usually virtual) vertical line which gives an energy denominator. The number of hole-particle pairs gives the excitation level.

As another example we consider the singly excited (i, a) component of the second-order wavefunction

$$-\frac{1}{2}\frac{E_i^a\,|\,\Phi_0\,\rangle}{\Delta_i^a}\sum_{b,j,k}\frac{\langle jk||ib\rangle\langle ab||jk\rangle}{\Delta_{jk}^{ab}} =$$

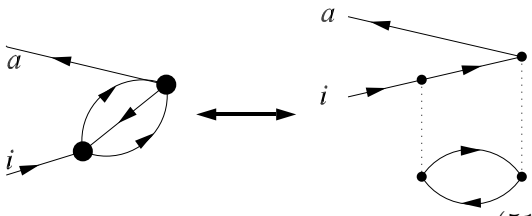

(51)

The factor 1/2 is due to the two equivalent internal hole lines in the Hugenholtz diagram and the minus sign to the loop ($l = 1$) and the two internal hole lines ($h = 2$) in the Brandow diagram. There are two imaginary vertical lines giving the energy denominators. The lines leaving the diagram are associated with

$$X_a^\dagger X_i\,|\,\Phi_0\,\rangle \equiv E_i^a\,|\,\Phi_0\,\rangle.$$

8 Coupled cluster Ansatz

In this section we will discuss that the exact, fully correlated, wavefunction Ψ can be written as

$$\Psi = e^T\,\Phi_0 \equiv \sum_{n=0}^{\infty}\frac{1}{n!}T^n\,\Phi_0$$

where Φ_0 is the Hartree-Fock ground state wavefunction and T is an operator to be introduced in this section. This manner of writing Ψ is known in the

literature as the coupled cluster "Ansatz". Ansatz is a German noun meaning something like "starting point".

So far we concentrated mainly on energies, not on wavefunctions, although we gave already two examples of correlated wavefunctions, Eqs. (50) and (51). We introduced (without proof) the *linked cluster theorem* for energies. This theorem is also valid for exact wavefunctions. It reads

$$| \Psi \rangle = \sum_{n=0}^{\infty} \{(RV)^n\}_{\rm L} \, | \Phi_0 \rangle, \tag{52}$$

where the subscript L indicates that the sum is only over linked wavefunction diagrams. Unfortunately, for a wavefunction diagram the adjective 'linked' does not mean the same as the adjective 'connected', whereas for an energy diagram the two are synonymous (as they are in daily life).

Definition:

A wavefunction diagram is unlinked if it contains one or more energy diagrams, otherwise it is linked.

(Remember that an energy diagram is closed, with no lines sticking out).

For example, the following wavefunction diagrams are both linked with the first one being connected and the second consisting of two connected pieces:

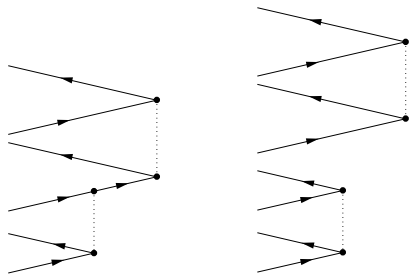

(53)

Both diagrams represent components of $\Phi^{(2)}$, the first one along a triply excited state and the second along a quadruply excited state. The following doubly excited fourth-order wavefunction diagram contains an energy contribution and hence is an example of an unlinked wavefunction contribution:

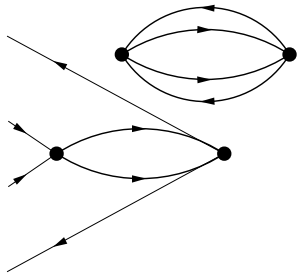

(54)

The linked cluster theorem states that Eq. (54) *does not* contribute to the exact wave function, whereas both terms in Eq. (53), the connected and the disconnected one, *do* contribute to Ψ.[1]

We will now turn to the cluster operator T. In order to explain its definition, we consider first the simple case of the full CI wavefunction of a four-electron closed-shell system. The exact wavefunction in intermediate normalization (i.e. the coefficient of the HF ground state is equal to unity) and written in summation convention is

$$\begin{aligned}\Psi &= \Phi_0 + c_a^i E_i^a \Phi_0 + c_{a_1a_2}^{i_1i_2} E_{i_1i_2}^{a_1a_2} \Phi_0 + c_{a_1a_2a_3}^{i_1i_2i_3} E_{i_1i_2i_3}^{a_1a_2a_3} \Phi_0 + c_{a_1a_2a_3a_4}^{i_1i_2i_3i_4} E_{i_1i_2i_3i_4}^{a_1a_2a_3a_4} \Phi_0 \\ &= (1 + C_1 + C_2 + C_3 + C_4)\Phi_0. \end{aligned} \tag{55}$$

Here we introduced the operator $C_k \equiv c_{a_1\cdots a_k}^{i_1\cdots i_k} E_{i_1\cdots i_k}^{a_1\cdots a_k}$, which contains the CI coefficients $c_{a_1\cdots a_k}^{i_1\cdots i_k}$, which have yet to be obtained from a full CI calculation. In a similar manner the following linear combination of all k-fold excited *connected* contributions to the exact wavefunction is introduced:

$$T_k \equiv \left(\frac{1}{k!}\right)^2 t_{a_1a_2\cdots a_k}^{i_1i_2\cdots i_k} E_{i_1i_2\cdots i_k}^{a_1a_2\cdots a_k}, \quad \text{for } k = 1, 2, \ldots, N. \tag{56}$$

The expansion coefficients ('cluster amplitudes') $t_{a_1a_2\cdots a_k}^{i_1i_2\cdots i_k}$ are the unknowns. Diagrammatic perturbation theory may be applied to obtain these coefficients, which are represented by connected diagrams only. For instance the first few T_2 terms are given in Fig. 1 as connected diagrams (schematic, many different arrow settings are possible, sum over the labels of the free particle-hole pairs is implied, the open circle with four free lines represents the exact $T_2 \,|\, \Phi_0 \,\rangle$). Thus, the first-order contribution $(t^{(1)})_{ab}^{ij}$ to the cluster amplitude t_{ab}^{ij}, which multiplies $E_{ij}^{ab} \,|\, \Phi_0 \,\rangle$:

$$(t^{(1)})_{ab}^{ij} = \langle ab||ij\rangle / \Delta_{ij}^{ab}.$$

[Note that the weight factor $1/4$ cancels against $(1/k!)^2$ in the definition of t_{ab}^{ij}].

The first contribution to T_1 (which starts at second-order) is given by the diagram in Eq. (51). Explicitly, the corresponding cluster amplitude is

$$\left(t^{(2)}\right)_a^i = -\frac{1}{2}\sum_{bjk} \frac{\langle jk||ib\rangle\langle ab||jk\rangle}{\Delta_i^a \Delta_{jk}^{ab}} + \frac{1}{2}\sum_{jcb} \frac{\langle aj||cb\rangle\langle cb||ij\rangle}{\Delta_i^a \Delta_{ij}^{bc}},$$

[1] Maybe 'linkable' would have been a better adjective for a wavefunction diagram than 'linked', since both diagrams in Eq. (53) can still lead to a single connected energy diagram, whereas the diagram in Eq. (54) is 'unlinkable' to a connected energy diagram.

Figure 1: *All perturbation contributions to T_2 through third order.*

$$T_2 \,|\, \Phi_0 \,\rangle \;=\; \approx \tag{57}$$

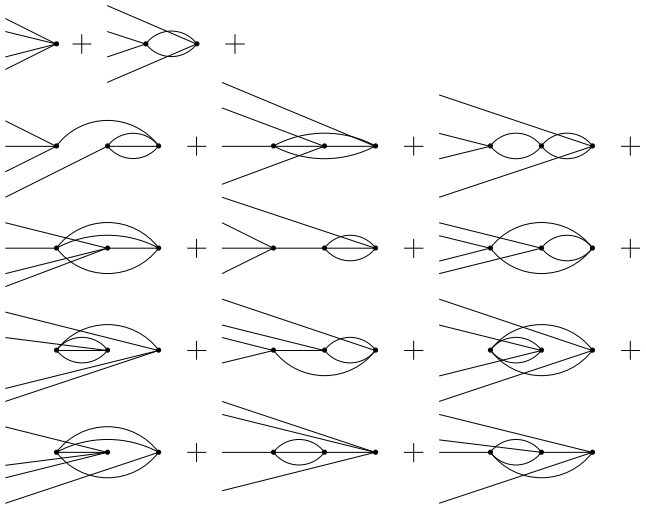

where the second term is due to a diagram of the same type as in Eq. (51), but with the arrows inverted on the fork labeled by a and i. The first contribution to T_3 is also of second-order and is given by the leftmost diagram in Eq. (53). We see here that perturbation theory gives the cluster amplitudes order by order. In the next section we will derive non-perturbative equations to obtain the cluster amplitudes. When we solve these equations iteratively diagrams of order n in the MP potential are added to the wavefunction in the nth iteration.

As stated before, the connected diagrams give only part of the exact wave function. Any linked disconnected diagram consisting of $n > 1$ pieces will contribute to Ψ as well. In appendix B we make plausible by considering all perturbation contributions that the exact wave function of an N-electron system may be written as an exponential operator acting on the Hartree-Fock ground state:

$$\boxed{|\,\Psi\,\rangle = e^T \,|\,\Phi_0\,\rangle} \tag{58}$$

with $T = T_1 + T_2 + \cdots T_N$. That is, the disconnected contributions are simply powers of the connected contributions T_1, T_2,..., T_N.

As an alternative to the perturbation theory approach of appendix B, we can obtain the exponential Ansatz from full CI. As an example we consider

again the four-electron closed shell system. It is easy to write out the exponential operator and upon sorting the terms with respect to excitation level the exact wavefunction becomes Eq. (55), in which the following substitutions are made:

$$\begin{aligned} C_1 &= T_1 \\ C_2 &= T_2 + \frac{1}{2}T_1^2 \\ C_3 &= T_3 + T_1T_2 + \frac{1}{6}T_1^3 \\ C_4 &= T_4 + T_1T_3 + \frac{1}{2}T_1^2T_2 + \frac{1}{2}T_2^2 + \frac{1}{24}T_1^4. \end{aligned} \tag{59}$$

The terms T_1, T_2, T_3 and T_4 are the connected contributions and all the remaining terms are disconnected (but linked, no energy diagrams multiply the wavefunction diagrams).

By inverting these equations we can formally show that the exponential Ansatz is true for the exact wavefunction. Inversion gives

$$\begin{aligned} T_1 &= C_1 \\ T_2 &= C_2 - \frac{1}{2}C_1^2 \\ T_3 &= C_3 - C_1C_2 + \frac{1}{3}C_1^3 \\ T_4 &= C_4 - C_1C_3 + C_1^2C_2 - \frac{1}{2}C_2^2 - \frac{1}{4}C_1^4. \end{aligned} \tag{60}$$

In these equations the disconnected parts are subtracted from C_n, so that T_n is a sum of connected pieces only ($n = 1, 2, 3, 4$). One easily verifies now, using $\ln(1+x) = \sum_{n=1} \frac{(-1)^{n-1}}{n} x^n$, that

$$T_1 + T_2 + T_3 + T_4 = \ln(1 + C_1 + C_2 + C_3 + C_4),$$

since higher than four-fold excitations vanish in a four-electron system. Hence

$$e^{T_1+T_2+T_3+T_4} \mid \Phi_0 \rangle = (1 + C_1 + C_2 + C_3 + C_4) \mid \Phi_0 \rangle \equiv \mid \Psi \rangle.$$

So, the exponential operator acting on the HF ground state wave function yields indeed the *exact* (full CI) wavefunction $\mid \Psi \rangle$. However, it is not rigorously proved in this procedure that $T_k \mid \Phi_0 \rangle$ is indeed represented by a sum of *connected* diagrams only; for the clarification of this we refer to Appendix B.

There is an interesting way of looking at the size extensivity of the coupled cluster Ansatz. Suppose our system consists of two noninteracting systems A and B ($H = H_A + H_B$), each with their own orbitals. The orbitals on A and B being orthogonal to each other, it is easily seen that the excitation operators on A and B commute and hence also the cluster operators. We write $T = T_A + T_B$ and from $[T_A, T_B] = 0$ we conclude that $\exp(T) = \exp(T_A)\exp(T_B)$. (This is not true if T_A does not commute with T_B!). Since the Hartree-Fock method is size extensive the HF wavefunction factorizes for two non-interacting systems: $\Phi_0 = \Phi_0^A \otimes \Phi_0^B$. Under these conditions the exact Ψ factorizes: $\Psi = \left[\exp(T_A)\Phi_0^A\right] \otimes \left[\exp(T_B)\Phi_0^B\right]$ and the corresponding energy is accordingly strictly additive.

9 Coupled cluster equations

The cluster operator T_k, Eq. (56), contains coefficients $t_{a_1 a_2 \cdots a_k}^{i_1 i_2 \cdots i_k}$, which we have introduced by their perturbation expansion. However, we can also formulate (non-linear) equations from which these coefficients can be determined; these are the coupled cluster equations. These CC equations can be seen as an algebraic means to sum certain classes of diagrams to infinite order.

9.1 Exact CC equations

We recall from elementary quantum mechanics the following theorem

$$e^{-A}\, B\, e^{A} = A + [B, A] + \frac{1}{2!}[[B, A], A] + \frac{1}{3!}[[[B, A], A], A] + \cdots \tag{61}$$

i.e. a Taylor expansion in commutators. Now, introducing $H_N \equiv H - \langle\, H \,\rangle$ and $\Delta E \equiv E - \langle\, H \,\rangle$ we may write the exact Schrödinger equation

$$H_N \Psi = \Delta E \Psi \Longrightarrow H_N e^T \Phi_0 = \Delta E e^T \Phi_0 \Longrightarrow e^{-T} H_N e^T \Phi_0 = \Delta E \Phi_0, \tag{62}$$

so that it takes the following interesting form:

$$\Big(H_N + [H_N, T] + \frac{1}{2!}[[H_N, T], T] + \frac{1}{3!}[[[H_N, T], T], T] + \frac{1}{4!}[[[[H_N, T], T], T], T] \Big) \Phi_0 = \Delta E \Phi_0. \tag{63}$$

The *commutator expansion stops after the fifth term* because H_N does not contain higher than two-body interactions.

In order to explain this truncation after five terms in (63) we work out in somewhat more detail the commutator $[U, T_2]$ where U is the one-electron operator defined in (43), which we now write in summation convention

$$U = u_p^q \, E_q^p \quad \text{with} \quad u_p^q \equiv \langle \, p \, | \, u \, | \, q \, \rangle.$$

We will show that in the case of one-particle operators the commutator expansion stops after three terms. The excitation operators in T_2 simply factorize $E_{i_1 i_2}^{a_1 a_2} = E_{i_1}^{a_1} E_{i_2}^{a_2}$. So we meet commutation relations of the type

$$[E_q^p, E_i^a] = \delta_q^a E_i^p - \delta_i^p E_q^a. \tag{64}$$

From the general rule

$$[A, BC] = [A, B]C + B[A, C]$$

we obtain the following expression

$$[E_q^p, E_{i_1 i_2}^{a_1 a_2}] \;\; = \;\; \delta_q^{a_1} E_{i_1 i_2}^{p a_2} + \delta_q^{a_2} E_{i_1 i_2}^{a_1 p} - \delta_{i_1}^p E_{q i_2}^{a_1 a_2} - \delta_{i_2}^p E_{i_1 q}^{a_1 a_2}. \tag{65}$$

Hence

$$[U, T_2] \;\; = \;\; t_{a_1 a_2}^{i_1 i_2} \Big[u_p^{a_1} E_{i_1 i_2}^{p a_2} + u_p^{a_2} E_{i_1 i_2}^{a_1 p} - u_{i_1}^q E_{q i_2}^{a_1 a_2} - u_{i_2}^q E_{i_1 q}^{a_1 a_2} \Big] \tag{66}$$

Note that the E's on the right hand side carry only one label (p or q) arising from U. In the integrals appearing in U the indices q and p are replaced by a's and i's, respectively, labels which arise from T_2. The singly nested commutation relation connects by one internal (summation) line U with T. To represent diagrammatically this equation we recall that four lines must be sticking out to the left when representing $E_{i_1 i_2}^{a_1 a_2} \, | \, \Phi_0 \, \rangle$ and the same holds for $E_{i_1 i_2}^{p a_2} \, | \, \Phi_0 \, \rangle$, provided p is a particle (virtual) orbital. (When p is a hole orbital it contracts to either i_1 or i_2 to obtain a nonvanishing ket and we are left with a single excitation operator). An open circle is associated with $t_{a_1 a_2}^{i_1 i_2}$; no energy denominator is implied. The black dot represents u_p^q. Assuming that p and q are a particle and hole orbital, respectively, we get the following diagrammatic representation of Eq. (66):

$[U, T_2] \, | \, \Phi_0 \, \rangle =$

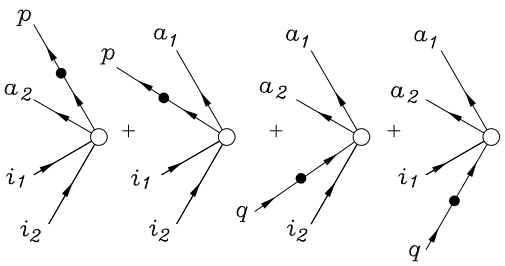

(67)

The minus signs in the last two terms are contained in the diagrams and follow from the presence of internal hole lines.

If we now consider the two-fold nested commutator $[[U,T_2],T_2]$ we meet as the first term

$$t^{i_1i_2}_{a_1a_2}t^{i_3i_4}_{a_3a_4}u^{a_1}_{p}\left[E^{pa_2}_{i_1i_2},E^{a_3a_4}_{i_3i_4}\right].$$

The commutator can be easily worked out when we recall that excitation operators commute

$$\begin{aligned}\left[E^{pa_2}_{i_1i_2},E^{a_3a_4}_{i_3i_4}\right] &= E^{p}_{i_1}\left[E^{a_2}_{i_2},E^{a_3a_4}_{i_3i_4}\right]+\left[E^{p}_{i_1},E^{a_3a_4}_{i_3i_4}\right]E^{a_2}_{i_2}\\ &= -(\delta^{p}_{i_3}E^{a_3a_4}_{i_1i_4}+\delta^{p}_{i_4}E^{a_3a_4}_{i_3i_1})E^{a_2}_{i_2}. \qquad (68)\end{aligned}$$

We see that no labels from U remain and that the surviving operators are all excitation operators. The same is true for the final operators arising from the other terms of Eq. (66), so that $[[[U,T_2],T_2],T_2]=0$ and the cluster expansion of a one-electron operator ends after three terms.

The two-fold nested commutator gives a connection of U with two T's, for instance the first term:

$$t^{i_1i_2}_{a_1a_2}t^{i_3i_4}_{a_3a_4}u^{a_1}_{i_3}E^{a_3a_4a_2}_{i_1i_4i_2}\,|\,\Phi_0\,\rangle =$$

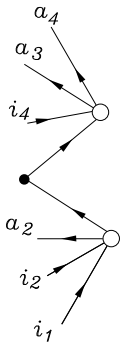

Turning now to two-electron operators we note that the operator appearing in the two-electron operator satisfies $E^{pq}_{rs}=E^{p}_{r}E^{q}_{s}-\delta^{q}_{r}E^{p}_{s}$ and has four free labels, p, q, r and s. In each level of nested commutation one of these labels is replaced by a hole or particle label originating from the T, just as in the one-electron operator case, so that no labels on the E^{p}_{q}'s arising from H_N remain after working out the fourfold nested commutator. The operator H_N is fully connected by four lines with one or more (up to four) T's. Only excitation operators are found in the four times nested commutator and since excitation operators commute, it follows that the five times nested commutator must be zero. Also in the lower commutators we find only excitation operators, as we act on the HF ground state in Eq. (63).

Since H_N is fully connected with the T's in Eq. (63) we introduce the short hand notation:

$$\{H_N T^n\}_{\rm C} \equiv [\cdots[H_N,T],\cdots,T] \qquad (n \text{ times } T), \tag{69}$$

so that by projection of Eq. (63) by $\langle\,\Phi_0\,|$ we get

$$\Delta E = \sum_{n=0}^{4} \frac{1}{n!} \langle\,\Phi_0\,|\,\{H_N T^n\}_{\rm C}\,|\,\Phi_0\,\rangle. \tag{70}$$

The exact correlation energy ΔE is written here as an expansion of connected quantities. It is important to observe that this expansion remains valid when we only include certain terms of T. As the energy expansion is solely in terms of connected (is the same as linked for energy) diagrams the energy stays size-extensive upon restriction of T.

For the moment we do not make any approximations and use that $\langle\,\Phi_0\,|T = 0$, so that in Eq. (63) only terms with the T's on the right of H_N are non-vanishing, hence we can also write

$$\Delta E = \sum_{n=0}^{4} \frac{1}{n!} \langle\,H_N\,T^n\,\rangle, \tag{71}$$

which in contrast to Eq. (70) is not manifestly connected. If we further use that the ket may be at most doubly excited to get a non-vanishing matrix element over a two-electron operator, together with the Brillouin theorem $\langle\,H_N T_1\,\rangle = t_a^i \langle\,H_N E_i^a\,\rangle = 0$ and $\langle\,H_N\,\rangle = 0$, we arrive at the following deceivingly simple looking expression for the *exact correlation* energy

$$\boxed{\Delta E = \langle\,H_N T_2\,\rangle + \frac{1}{2}\langle\,H_N T_1^2\,\rangle.} \tag{72}$$

The coupled cluster equations for the cluster amplitudes (hidden in T) are obtained by projection of Eq. (63) onto k-fold excited states,

$$\boxed{\sum_{n=0}^{4} \frac{1}{n!} \langle\,\Phi_{i_1\cdots i_k}^{a_1\cdots a_k}\,|\,\{H_N T^n\}_{\rm C}\,|\,\Phi_0\,\rangle = 0,} \tag{73}$$

where we used that $\langle\,\Phi_{i_1\cdots i_k}^{a_1\cdots a_k}\,|\,\Phi_0\,\rangle \equiv \langle\,E_{i_1\cdots i_k}^{a_1\cdots a_k}\Phi_0\,|\,\Phi_0\,\rangle = 0$.

9.2 The CCD equations

Equations (72) and (73) are the exact coupled cluster equations, which are equivalent to the exact Schrödinger equation. In order to solve them approximations must be introduced. The simplest approximation is the CCD approach [referred to as coupled pair many electron theory (CPMET) by its inventors Čížek and Paldus]

$$T \approx T_2 = E^{ab}_{ij}\, t^{ij}_{ab}$$

(summation convention!). Projection onto the doubles gives the CCD equations [take $k = 2$ in Eq. (73)], where summation over repeated superscripts and subscripts is again implied (a, b, i, and j are fixed labels):

$$\begin{aligned} 0 &= \langle\, \Phi^{ab}_{ij} \,|\, H_N \,|\, \Phi_0 \,\rangle + \langle\, \Phi^{ab}_{ij} \,|\, \{H_N E^{a_1a_2}_{i_1i_2}\}_{\rm C} \,|\, \Phi_0 \,\rangle t^{i_1i_2}_{a_1a_2} \\ &+ \frac{1}{2}\langle\, \Phi^{ab}_{ij} \,|\, \{H_N E^{a_1a_2}_{i_1i_2} E^{a_3a_4}_{i_3i_4}\}_{\rm C} \,|\, \Phi_0 \,\rangle t^{i_1i_2}_{a_1a_2} t^{i_3i_4}_{a_3a_3}. \end{aligned} \tag{74}$$

Note that these equations have the following structure

$$0 = A_k + \sum_{l=1}^{M} B_{kl}\, x_l + \sum_{l,l'}^{M} C_{kll'}\, x_l x_{l'}, \quad \text{with} \quad k = 1, \ldots, M,$$

and where $M = n^2_{\rm nocc} n^2_{\rm vir}$. We have as many unknowns M (the amplitudes $x_l \equiv t^{ij}_{ab}$) as equations and accordingly the t's can be solved from this set of coupled quadratic equations. Since we are projecting onto the doubles the connected diagrams must also have four lines (marked by i, j, a, b) sticking out to the left. [We must multiply Eq. (74) by $|\, \Phi^{ab}_{ij} \,\rangle$ to enable the diagrammatic representation].

In order to indicate how diagrams may be used to reduce Eq. (74) to an equation containing only one- and two-electron integrals, we first consider the one-electron contributions to the term linear in $t^{i_1i_2}_{a_1a_2}$. The operator H_N contains a one-electron operator, which we indicated by a small dot, and we saw before that $\sum_{a_1} \langle\, p \,|\, u \,|\, a_1 \,\rangle t^{ij}_{a_1b}$ and $\sum_{i_1} \langle\, i_1 \,|\, u \,|\, q \,\rangle t^{i_1j}_{ab}$, etc., arise. Contraction within the two-electron part of H_N is possible, i.e. terms of the type $\sum_{a_1} t^{ij}_{a_1b} \sum_k \langle ak||a_1k\rangle$ appear. These are the loops in the following diagrams:

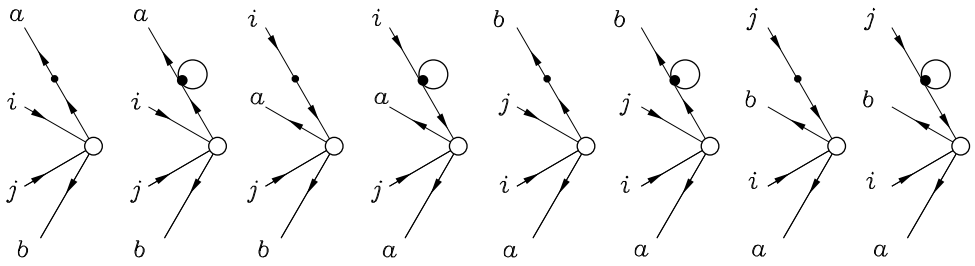

Using canonical HF orbitals, that is, $\langle\, a \,|\, u \,|\, a_1 \,\rangle + \sum_k \langle ak||a_1k\rangle = \epsilon_a \delta_{aa_1}$, we find that these eight diagrams give

$$(\epsilon_a - \epsilon_i + \epsilon_b - \epsilon_j) t_{ab}^{ij} \,|\, \Phi_{ij}^{ab} \,\rangle \equiv -\Delta_{ij}^{ab} t_{ab}^{ij} \,|\, \Phi_{ij}^{ab} \,\rangle. \tag{75}$$

The fact that no powers in the t's higher than two appear in the CCD approximation is most easily seen diagrammatically. The non-HF diagrams appearing in Eq. (74) are very schematically:

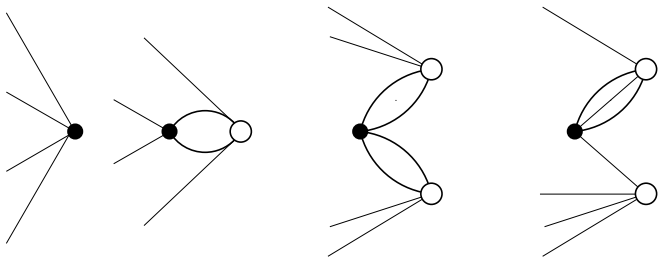

(76)

The first diagram represents simply $|\, \Phi_{ij}^{ab} \,\rangle\langle\, \Phi_{ij}^{ab} \,|\, H_N \,|\, \Phi_0 \,\rangle = |\, \Phi_{ij}^{ab} \,\rangle\langle ij||ab\rangle$. In the second diagram H_N and T_2 are connected by two lines. The last two diagrams are quadratic in T_2. Note now that it is impossible to have a contribution containing the third power T_2^3 that is connected with H_N and has four free lines.

By bringing Eq. (75) to the left hand side of Eq. (74), dividing both sides by Δ_{ij}^{ab} and summing over i, j, a, b, we can rewrite Eq. (74) in a form suitable for iteration

$$T_2 \,|\, \Phi_0 \,\rangle = R_2 \Big[V_N + \{V_N T_2\}_{\rm C} + \frac{1}{2} \{V_N T_2^2\}_{\rm C} \Big] \,|\, \Phi_0 \,\rangle, \tag{77}$$

where the resolvent R_2 on the space of 2-fold excited states (sum over repeated indices is implied) is defined for general k

$$R_k = \frac{E_{i_1 \cdots i_k}^{a_1 \cdots a_k} \,|\, \Phi_0 \,\rangle\langle\, \Phi_0 \,| E_{a_1 \cdots a_k}^{i_1 \cdots i_k}}{\Delta_{i_1 \cdots i_k}^{a_1 \cdots a_k}}.$$

This definition is a specialization of the more general reduced resolvent introduced in Eq. (11).

We reiterate that the appearance of the orbital energies is due to the fact that we used canonical HF orbitals. It can be proved, more rigorously than is done here, that no other one-electron terms than the orbital energies arise when canonical SCF orbitals are used. This proof shows that only the two-electron operator $V_N \equiv H_N - F$ appears on the right hand side of Eq. (77).

Note parenthetically that $V_N = V - \langle F \rangle$, where V is the Møller-Plesset operator defined in Eq. (21).

We end here the outline of the fact that it is possible to reduce the N-electron CCD equations Eq. (74) to orbital equations by the diagrammatic rules given above. That is, matrix elements as, for example, $\langle \Phi_{ij}^{ab} \,|\, \{V_N T_2\}_{\rm C} \,|\, \Phi_0 \rangle$ can be expressed in terms of one- and two-electron integrals and cluster amplitudes. Orbital equations can be found in the literature for CCD ($T \approx T_2$), CCSD ($T \approx T_1 + T_2$) and for CCSDT ($T \approx T_1 + T_2 + T_3$).

9.3 CC theory versus MP theory

The fact that coupled cluster theory sums certain Møller-Plesset diagrams to infinite order can be shown by noting that the CC equations may be solved iteratively. In each iteration a perturbation order is added. In Appendix B we went from MP to CC, we will now give a rough sketch of how to go from CC back to MP. We illustrate this on the CCD equations [Eq. (77)] and drop the suffix C. It is understood that from now on only connected terms are considered. The iteration is started by putting T_2 on the right hand side equal to zero, hence

$$T_2^{(1)} \,|\, \Phi_0 \rangle = R_2 V_N \,|\, \Phi_0 \rangle.$$

This confirms that T_2 starts with a first-order (in V_N) term. If we insert this into the coupled cluster energy, Eq. (72), and realize that only V_N gives a contribution, we get

$$E^{(2)} = \langle V_N R_2 V_N \rangle = \langle V R_2 V \rangle,$$

which is the second-order MP energy, cf. Eq. (22). Insert $T_2^{(1)}$ on the right hand side of Eq. (77) and we get the second-order contribution:

$$T_2^{(2)} \,|\, \Phi_0 \rangle = R_2 V_N R_2 V_N \,|\, \Phi_0 \rangle,$$

yielding the third-order MP energy. Third-order contributions to T_2 arise from $R_2 V_N R_2 V_N R_2 V_N$ and $1/2 R_2 V_N (R_2 V_N)^2$. The first term gives simply a fourth-order energy diagram with intermediate doubles [see Eq. (78)], while the second term gives the diagram on the right with short denominators on the part that has the quadruply excited intermediates

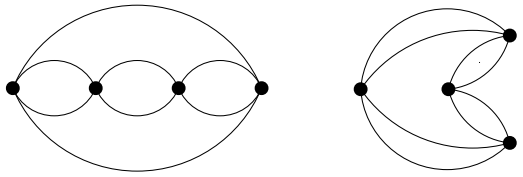

(78)

We can now use the factorization lemma (see Appendix B) in opposite direction and find that the second diagram is the sum of two connected MP diagrams with doubly and quadruply intermediate excited states. Inclusion of T_2 in the CC approach gives energy diagrams that in the CI approach would require quadruply excited states. One can continue the iteration and thus effectively sum the MP series for certain kinds of diagrams.

9.4 CCSD(T)

In the MP4 energy we find diagrams with intermediate triples, these do not occur in CCD. Neither the MP4 energy diagrams with intermediate singles appear in CCD, however CCSD will generate the latter. An example of a fourth-order diagram with intermediate triples, missed out by CCSD, is

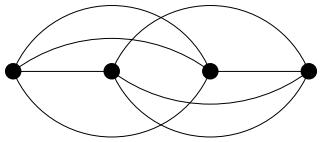

(79)

Suppose now that the CCSD equations have been solved exactly, so that the converged solutions $\overline{T}_1$ and $\overline{T}_2$ are known, which diagrammatically are designated by open circles with two and four free lines, respectively. Then we can approximate T_3 by $R_3 V_N \overline{T}_2$, i.e.

$T_3 \,|\, \Phi_0 \,\rangle \approx$ 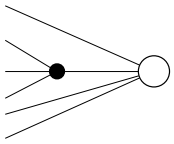

(80)

and compute the energies $\langle \, \{\overline{T}_2^\dagger V_N T_3\}_{\rm C} \,\rangle$ and $\langle \, \{\overline{T}_1^\dagger V_N T_3\}_{\rm C} \,\rangle$ represented by diagrams of the type

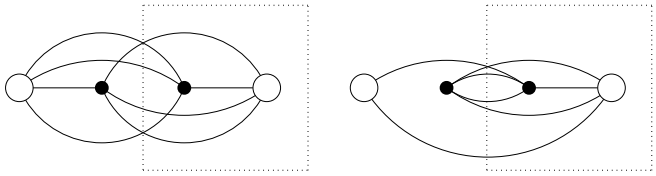

(81)

where the subdiagram within the dashed boxes represent $T_3 \,|\, \Phi_0 \,\rangle$. This is the CCSD(T) method. The solution of the CCSD equations scales with the number of orbitals n as $n^6 N_{\rm iter}$. Obviously Eq. (80), the computation of the non-iterative T_3, scales as n^7. Therefore the CCSD(T) method is often used as a cheaper alternative to CCSDT, where the equations (73) for $k = 1, 2, 3$

are solved simultaneously and which scales as $n^8 N_{\text{iter}}$. Since T_2 starts in first-order, the lowest order contribution to the first diagram in Eq. (81) is just the MP4 diagram of Eq. (79). Since T_1 is of second-order the lowest order of the second diagram in Eq. (81) is the MP5 diagram (Hugenholtz and one of its Goldstone representatives):

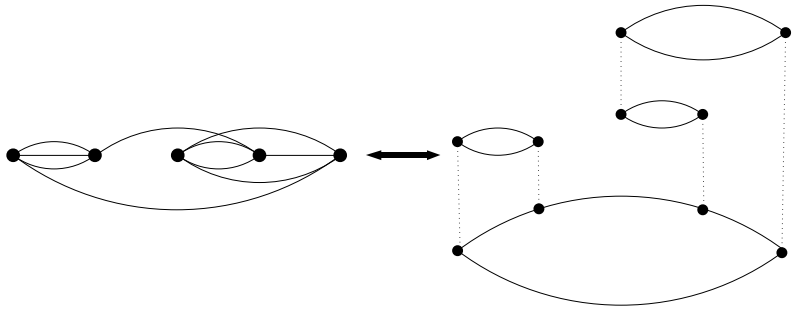

(82)

In other words, CCSD(T) not only accounts for 4^{th}-order diagrams with intermediate triples, but also contains quite a number of 5^{th}-order contributions. Since CCSD(T) is not much more expensive than MP4, it explains why CCSD(T) has become a widely applied correlation method.

A Hartree-Fock, Slater-Condon, Brillouin

We write a normalized N-electron Slater determinant Φ_0 with the aid of the antisymmetrizer $\mathcal{A} \equiv \frac{1}{N!} \sum_{P \in S_N} (-1)^p P$, where S_N is the group containing all permutations P of N electrons and $(-1)^p$ is the parity of P.

$$\Phi_0 = \sqrt{N!}\, \mathcal{A}\, \psi_{i_1} \psi_{i_2} \cdots \psi_{i_N} \equiv \{\psi_{i_1} \psi_{i_2} \cdots \psi_{i_N}\}$$

Normalized Slater determinants will be designated by curly brackets. The variation of

$$E_{\text{HF}} \equiv \langle\, \Phi_0 \,|\, H \,|\, \Phi_0 \,\rangle$$

with the constraint that $\langle\, \psi_i \,|\, \psi_j \,\rangle = \delta_{ij}$ leads to the one-electron eigenvalue equation (HF equation)

$$f(1)\psi_p(1) = \epsilon_p \psi_p(1)$$

with

$$f(1) = u(1) + \sum_{i=1}^{N} \langle\, \psi_i(2) \,|\, (1 - P_{12})/r_{12} \,|\, \psi_i(2) \,\rangle \tag{83}$$

The bracket denotes an integral over space and spin coordinates of electron 2. The operator P_{12} permutes space and spin coordinates of electron 1 and 2.

The one-electron Fock operator f has in principle an infinite set of eigenvalues and eigenvectors.

We introduce the notation $\langle\, p \,|\, u \,|\, q \,\rangle$ for $\langle\, \psi_p \,|\, u \,|\, \psi_q \,\rangle$ and $\langle pq||rs\rangle$, which is shorthand for $\langle\, \psi_p(1)\psi_q(2) \,|\, (1-P_{12})/r_{12} \,|\, \psi_r(1)\psi_s(2) \,\rangle$.

The N-electron Fock operator $F \equiv \sum_{i=1}^{N} f(i)$ commutes with $\mathcal{A}$, i.e. $\mathcal{A}F = F\mathcal{A}$. Noting that by definition a canonical orbital $\psi_{p_i}(i)$ satisfies $f(i)\psi_{p_i}(i) = \epsilon_{p_i}\psi_{p_i}(i)$, it follows easily that a Slater determinant containing canonical HF orbitals is an eigenfunction of F. Indeed,

$$\begin{aligned} F\,\{\psi_{p_1}(1)\cdots\psi_{p_N}(N)\} &\equiv \sqrt{N!}\,F\,\mathcal{A}\psi_{p_1}(1)\cdots\psi_{p_N}(N) \\ &= \sqrt{N!}\,\mathcal{A}\sum_{i=1}^{N} f(i)\;\psi_{p_1}(1)\cdots\psi_{p_N}(N) \\ &= \sqrt{N!}\,\mathcal{A}\Big(\sum_{i=1}^{N}\epsilon_{p_i}\Big)\psi_{p_1}(1)\cdots\psi_{p_N}(N) \\ &= \Big(\sum_{i=1}^{N}\epsilon_{p_i}\Big)\,\{\psi_{p_1}(1)\cdots\psi_{p_N}(N)\} \end{aligned} \tag{84}$$

Evidently, the subtraction of the constant

$$\langle\, H - F \,\rangle = E_{\rm HF} - \sum_{i=1}^{N}\epsilon_i = -\frac{1}{2}\sum_{i,j=1}^{N}\langle ij||ij\rangle \tag{85}$$

shifts the energies by this amount, but leaves the fact intact that Slater determinants are eigenfunctions of F.

In the main text we will need the Slater-Condon rules. These rules express matrix elements of one- and two-electron operators with Slater determinants in bra and ket in terms of one- and two-electron integrals. The orbitals appearing in bra and ket are orthogonal to each other and normalized. They are not necessarily canonical HF orbitals. First we apply a so-called *line-up* permutation $\mathcal{L}$ in the ket to bring orbitals in bra and ket to the same positions. Example for 5 electrons:

$$\langle\, \psi_1\psi_2\psi_3\psi_4\psi_6 \,|\, H \,|\, (312)\psi_3\psi_1\psi_2\psi_4\psi_5 \,\rangle = \langle\, \psi_1\psi_2\psi_3\psi_4\psi_6 \,|\, H \,|\, \psi_1\psi_2\psi_3\psi_4\psi_5 \,\rangle$$

Since $\mathcal{A}\mathcal{L} = (-1)^l\mathcal{A}$, where $(-1)^l$ is the parity of $\mathcal{L}$, we get at most a minus sign from applying the line-up permutation. In the example $\mathcal{L} = (123)$, which has parity $+1$. Note that the orbitals ψ_5 and ψ_6 are mismatching in bra and ket. From here on we assume that the orbitals are lined up and omit the possible minus sign.

The Slater-Condon rules distinguish four cases differing in the number of orbitals that mismatch between bra and ket.

- *0 mismatches*

  One-particle operator:

$$\langle \{\psi_{p_1}\psi_{p_2}\cdots\psi_{p_N}\} \mid \sum_{i=1}^{N} u(i) \mid \{\psi_{p_1}\psi_{p_2}\cdots\psi_{p_N}\} \rangle = \sum_{i=1}^{N} \langle p_i \mid u \mid p_i \rangle$$

  Two particle operator:

$$\langle \{\psi_{p_1}\psi_{p_2}\cdots\psi_{p_N}\} \mid \frac{1}{2}\sum_{i\neq j}^{N} \frac{1}{r_{ij}} \mid \{\psi_{p_1}\psi_{p_2}\cdots\psi_{p_N}\} \rangle = \frac{1}{2}\sum_{i,j}^{N} \langle p_i p_j || p_i p_j \rangle$$

- *1 mismatch*

  Suppose in position i we have

$$\langle \psi_{p_i}(i) \mid = \langle \psi_p(i) \mid, \quad \mid \psi_{p_i}(i) \rangle = \mid \psi_q(i) \rangle \text{ and } \psi_p(i) \neq \psi_q(i).$$

  One-particle operator:

$$\langle \{\psi_{p_1}\psi_{p_2}\cdots\psi_{p_N}\} \mid \sum_{i=1}^{N} u(i) \mid \{\psi_{p_1}\psi_{p_2}\cdots\psi_{p_N}\} \rangle = \langle p \mid u \mid q \rangle$$

  Two particle operator:

$$\langle \{\psi_{p_1}\psi_{p_2}\cdots\psi_{p_N}\} \mid \frac{1}{2}\sum_{i\neq j}^{N} \frac{1}{r_{ij}} \mid \{\psi_{p_1}\psi_{p_2}\cdots\psi_{p_N}\} \rangle = \sum_{j=1}^{N} \langle p\ p_j || q\ p_j \rangle$$

- *2 mismatches*

  Suppose in position i we have

$$\langle \psi_{p_i}(i) \mid = \langle \psi_p(i) \mid, \quad \mid \psi_{p_i}(i) \rangle = \mid \psi_q(i) \rangle \text{ and } \psi_p(i) \neq \psi_q(i).$$

  and for position j

$$\langle \psi_{p_j}(j) \mid = \langle \psi_r(j) \mid, \quad \mid \psi_{p_j}(j) \rangle = \mid \psi_s(j) \rangle \text{ and } \psi_r(j) \neq \psi_s(j).$$

  One-particle operator:

$$\langle \{\psi_{p_1}\psi_{p_2}\cdots\psi_{p_N}\} \mid \sum_{i=1}^{N} u(i) \mid \{\psi_{p_1}\psi_{p_2}\cdots\psi_{p_N}\} \rangle = 0$$

  Two particle operator:

$$\langle \{\psi_{p_1}\psi_{p_2}\cdots\psi_{p_N}\} \mid \frac{1}{2}\sum_{i\neq j}^{N} \frac{1}{r_{ij}} \mid \{\psi_{p_1}\psi_{p_2}\cdots\psi_{p_N}\} \rangle = \langle p\ r || q\ s \rangle$$

- *More than 2 mismatches*
  One-particle operator:

$$\langle \{\psi_{p_1}\psi_{p_2}\cdots\psi_{p_N}\} \mid \sum_{i=1}^{N} u(i) \mid \{\psi_{p_1}\psi_{p_2}\cdots\psi_{p_N}\} \rangle = 0$$

  Two particle operator:

$$\langle \{\psi_{p_1}\psi_{p_2}\cdots\psi_{p_N}\} \mid \frac{1}{2}\sum_{i\neq j}^{N} \frac{1}{r_{ij}} \mid \{\psi_{p_1}\psi_{p_2}\cdots\psi_{p_N}\} \rangle = 0$$

In the main text we will need Brillouin's theorem. This states that

$$\langle \Phi_0 \mid H \mid \Phi_i^a \rangle = \langle i \mid u \mid a \rangle + \sum_{j=1}^{N} \langle ip_j||ap_j\rangle = \langle i \mid f \mid a \rangle = 0,$$

provided ψ_i and ψ_a are canonical HF orbitals. The singly excited state Φ_i^a is obtained by replacing in Φ_0 the occupied spin-orbital i by the virtual spin-orbital a.

B Exponential structure of the wavefunction

We will outline how one can prove the exponential Ansatz for the wave function. The proof needs the factorization lemma of Frantz and Mills. Before we state this lemma we consider first an example of a factorization of the kind described by it.

The simplest linked disconnected diagram which appears in the exact wavefunction is the first diagram on the left hand side:

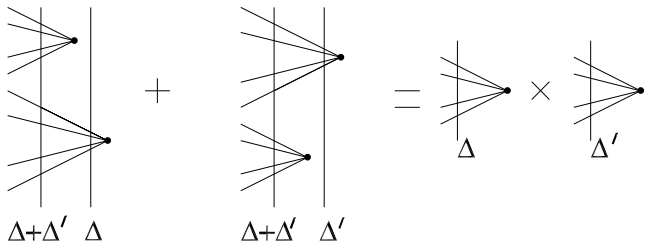

(86)

The two diagrams on the left hand side are equal. Diagrammatically this is obvious because the vertices are moved vertically and algebraically we have

$$\sum_{i,j,a,b}\sum_{i',j',a',b'} \frac{\langle ab||ij\rangle\langle a'b'||i'j'\rangle}{(\Delta_{ij}^{ab}+\Delta_{i'j'}^{a'b'})\Delta_{ij}^{ab}} E_{ij}^{ab}E_{i'j'}^{a'b'} \mid \Phi_0 \rangle$$

$$= \sum_{i',j',a',b'}\sum_{i,j,a,b} \frac{\langle a'b'||i'j'\rangle\langle ab||ij\rangle}{(\Delta_{ij}^{ab}+\Delta_{i'j'}^{a'b'})\Delta_{i'j'}^{a'b'}}, E_{i'j'}^{a'b'}E_{ij}^{ab} \mid \Phi_0 \rangle. \qquad (87)$$

By summing the two equal terms in this equation and multiplying by 1/2 we obtain the factorization

$$\sum_{i,j,a,b}\sum_{i',j',a',b'}\frac{\langle ab||ij\rangle\langle a'b'||i'j'\rangle E_{ij}^{ab}E_{i'j'}^{a'b'}}{(\Delta_{ij}^{ab}+\Delta_{i'j'}^{a'b'})\Delta_{ij}^{ab}}\,|\,\Phi_0\,\rangle$$

$$= \frac{1}{2}\left(\sum_{i,j,a,b}\frac{\langle ab||ij\rangle E_{ij}^{ab}}{\Delta_{ij}^{ab}}\right)\left(\sum_{i',j',a',b'}\frac{\langle a'b'||i'j'\rangle E_{i'j'}^{a'b'}}{\Delta_{i'j'}^{a'b'}}\right)\,|\,\Phi_0\,\rangle. \qquad (88)$$

This factorization is illustrated in Eq. (86). We see that by summing over two diagrams with equal numerators and different 'long denominators' (the vertical lines) we obtain a single product of diagrams with 'short denominators', this is half the square of the first-order contribution to T_2, namely $\frac{1}{2}\big(T_2^{(1)}\big)^2$. Here we have the simplest application of the Frantz-Mills lemma: the application to two equal subdiagrams, each containing one vertex.

In general, if we have one subdiagram with n vertices and one subdiagram with m vertices, then we have in total $(n+m)!/n!m!$ time versions of the compound diagram obtained by shifting the two subdiagrams with respect to each other along the horizontal axis. These time versions have the same numerators but different long denominators. The Frantz-Mills factorization lemma states now that the sum of the $(n+m)!/n!m!$ long denominators can be factorized into a product of short denominators. Since the numerator is by definition already a product, the sum of $(n+m)!/n!m!$ diagrams becomes algebraically a single product. So, in the perturbation expansion of the wavefunction sums of different time versions can be replaced by products. The factorization lemma is proved by mathematical induction. If we were to give a formal proof of the CC Ansatz, we would also have to use induction. However, we only sketch the beginning of this proof.

Let us consider as another example the case $n = 1$, $m = 2$, for instance the sum of the three third-order disconnected wavefunction diagrams on the left hand side:

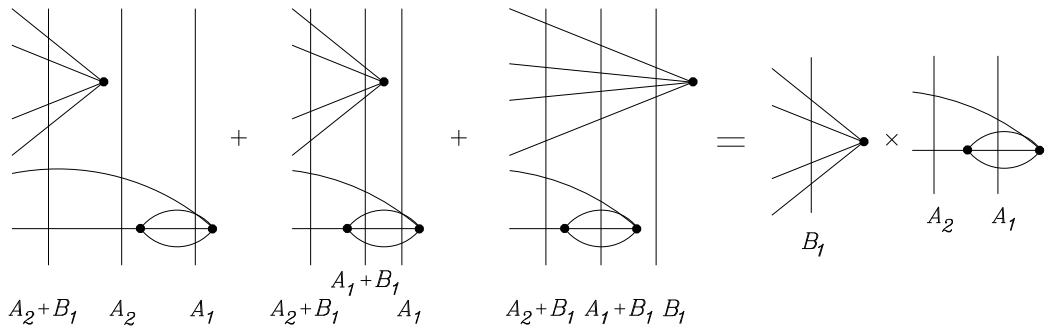

The numerators are equal and the denominators become

$$\frac{1}{A_2+B_1}\Big[\frac{1}{A_2A_1}+\frac{1}{(A_1+B_1)A_1}+\frac{1}{(A_1+B_1)B_1}\Big]=\frac{1}{A_1A_2B_1}. \tag{89}$$

Hence the sum of these three wavefunction diagrams factorizes and yields $T_2^{(1)}T_1^{(2)}$. In the very same way we obtain $T_2^{(1)}T_2^{(2)}$ from the sum of three diagrams with equal numerators.

As a further illustration we may consider the sum of the following six ($n=m=2$) schematic fourth-order diagrams all having the same numerator and consisting of two connected pieces:

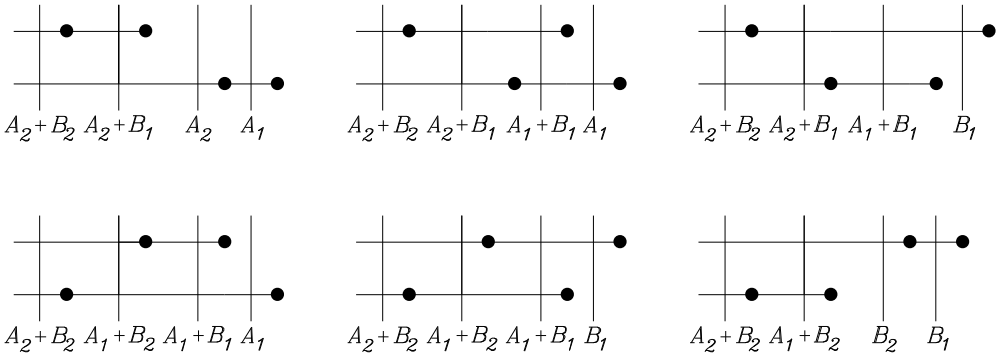

and the corresponding algebraic equation indeed factorizes:

$$\begin{aligned}
&\frac{1}{A_2+B_2}\Big[\frac{1}{(A_2+B_1)A_2A_1}+\frac{1}{(A_2+B_1)(A_1+B_1)A_1}\\
&+\frac{1}{(A_2+B_1)(A_1+B_1)B_1}+\frac{1}{(A_1+B_2)(A_1+B_1)A_1}+\\
&\frac{1}{(A_1+B_2)(A_1+B_1)B_1}+\frac{1}{(A_1+B_2)B_2B_1}\Big]\\
=\;&\frac{1}{A_1A_2B_1B_2}.
\end{aligned} \tag{90}$$

If the upper subdiagram is equal to the lower, for instance both subdiagrams are $T_1^{(2)}$ or $T_2^{(2)}$, then we overcount. The first diagram is then equal to the sixth, the second to the fifth and third is equal to the fourth. So in that case only three of the time versions are different, and we must divide by two (=2!). If the two subdiagrams are different, for instance the subdiagrams correspond to $T_1^{(2)}$ and $T_2^{(2)}$, respectively, then all six time versions are different and no division by two must be performed.

In summary, we found so far the following factorized terms

$$\begin{aligned}
&\frac{1}{2}\Big[\big(T_2^{(1)}\big)^2+\big(T_2^{(2)}\big)^2+\big(T_1^{(2)}\big)^2\Big]+T_2^{(1)}T_1^{(2)}+T_2^{(1)}T_2^{(2)}+T_1^{(2)}T_2^{(2)}\\
=\;&\frac{1}{2}\Big[T_1^{(2)}+T_2^{(1)}+T_2^{(2)}\Big]^2\approx\frac{1}{2}[T_1+T_2]^2.
\end{aligned} \tag{91}$$

Continuing in this manner, using the perturbation expansion of the k-cluster operator $T_k = \sum_n T_k^{(n)}$ and $T = \sum_k T_k$ we see that $\frac{1}{2}T^2$ is contained in the linked cluster expansion of the wavefunction.

Also linked wavefunction diagrams consisting of three subdiagrams connected by long denominators appear in the linked cluster expansion of the wavefunction. It can be shown that summing all time versions leads to a factorization of the long denominators. If the three subdiagrams are equal we have to correct for the fact that we overcount. Hence also $\frac{1}{3!}T^3 \,|\, \Phi_0 \,\rangle$ is contained in the linked cluster expansion. Continuing this argument, we find

$$\begin{aligned} |\, \Psi \,\rangle &= \sum_{n=0}^{\infty} \{(RV)^n\}_{\rm L} \,|\, \Phi_0 \,\rangle \\ &= (1 + T + \frac{1}{2!}T^2 + \frac{1}{3!}T^3 + \cdots) \,|\, \Phi_0 \,\rangle = e^T \,|\, \Phi_0 \,\rangle. \end{aligned} \tag{92}$$

So, we have made plausible that the exact wavefunction can be written in exponential form.

C Bibliography

The single most important reference to the above is unfortunately unpublished: J. Paldus, *Diagrammatic Methods for Many-Fermion Systems*, Lectures Notes, the University of Nijmegen, (1981). Here one finds all the proofs omitted in the present notes. A recent review paper by Paldus (together with X. Li) is: *A critical assessment of coupled cluster method in quantum chemistry*. It appeared in Adv. Chem. Phys. 1-175 **110** (1999).

Another important reference is *Time-Independent Diagrammatic Approach to Perturbation Theory of Fermion Systems* by J. Paldus and J. Čížek, Adv. Quantum Chem. **9**, 106 (1975). For obvious reasons Paldus's 1981 lecture notes leaned heavily on this work.

A recent review of CC theory is: R. J. Bartlett *Coupled-Cluster Theory: An Overview of Recent Developments* in: *Modern Electronic Structure Theory* Part II. Editor: D. R. Yarkony, World Scientific, Singapore (1995).

Two historic papers are: *Derivation of the Brueckner many-body theory* by J. Goldstone, Proc. Roy. Soc. (London) **A239**, 267 (1957) and *Perturbation Theory of Large Quantum Systems* by N. M. Hugenholtz, Physica **23**, 481 (1957).

The first derivation of the CCD equations for use in chemistry is by J. Čížek *(On the Correlation Problem in Atomic and Molecular Systems. Calculation of Wavefunction Components in Ursell-Type Expansion Using Quantum-Field Theoretical Methods)*, J. Chem. Phys. **45**, 4256 (1966). General diagrammatic rules were given.

The CCSD equations were derived by G. D. Purvis and R. J. Bartlett (using the Čížek rules) J. Chem. Phys. **76**, 1910 (1982) in a paper entitled: *A full coupled-cluster singles and doubles model: The inclusion of disconnected triples.* (By 'disconnected triples' the authors refer to T_1T_2 and T_1^3).

The CCSDT equations appeared in Adv. Quantum Chem. **18**, 207 (1986): M. R. Hoffmann and H. F. Schaefer *A Full Coupled-Cluster Singles, Doubles, and Triples Model for the Description of Electron Correlation.*

The CCSD(T) model was introduced by K. Raghavachari, G. W. Trucks, J. A. Pople, and M. Head-Gordon, Chem. Phys. Lett.. **157**, 479 (1989). Title: *A fifth-order perturbation comparison of electron correlation theories.*

All fourth-order MP diagrams can be found in: R. J. Bartlett and G. D. Purvis, Int. J. of Quantum Chem. **14**, 561 (1978) or S. Wilson and D. M. Silver, Int. J. of Quantum Chem. **15**, 683 (1979).

Finally, the following textbook has a clear chapter on MP theory: A. Szabo and N. S. Ostlund, *Modern Quantum Chemistry: Introduction to Advanced Electronic Structure Theory*, MacMillan, New York (1982).